Organic & Biomolecular Chemistry

Cite this: *Org. Biomol. Chem.*, 2011, **9**, 6422

www.rsc.org/obc

PAPER

Impact of planarity of unfused aromatic molecules on G-quadruplex binding: Learning from isaindigotone derivatives†

Jin-Qiang Hou, Jia-Heng Tan, Xiao-Xiao Wang, Shuo-Bin Chen, Si-Yuan Huang, Jin-Wu Yan, Shu-Han Chen, Tian-Miao Ou, Hai-Bin Luo, Ding Li, Lian-Quan Gu* and Zhi-Shu Huang*

Received 3rd June 2011, Accepted 20th June 2011
DOI: 10.1039/c1ob05884c

G-quadruplex structures are a new class of attractive targets for DNA-interactive anticancer agents. The primary building block of this structure is the G-quartet, which is composed of four coplanar guanines and serves as the major binding site for small molecules. NMR studies and molecular dynamics simulations have suggested that the planarity of G-quartet surface has been highly dynamic in solution. To better investigate how the planarity of unfused aromatic ligand impacts on its quadruplex binding properties, a variety of planarity controllable isaindigotone derivatives were designed and synthesized. The interaction of G-quadruplex DNA with these designed ligands was systematically explored using a series of biophysical studies. The FRET-melting, SPR, and CD spectroscopy results showed that reducing the planarity of their unfused aromatic core resulted in their decreased binding affinity and stabilization ability for G-quadruplex. NMR studies also suggested that these compounds could stack on the G-quartet surface. Such results are in parallel with subsequent molecular modeling studies. A detailed binding energy analysis indicated that van der Waals energy (ΔE_{vdw}) and entropy ($T\Delta S$) are responsible for their decreased quadruplex binding and stabilization effect. All these results provided insight information about how quadruplex recognition could be controlled by adjusting the planarity of ligands, which shed light on further development of unfused aromatic molecules as optimal G-quadruplex binding ligands.

Introduction

The guanine-rich single strand can adopt higher-order structures called the G-quadruplexes under appropriate cation conditions.[1–3] The primary building block of this structure is the π-stacked G-quartets, each of which is connected by a network of eight Hoogsteen hydrogen bonds. Possible G-quadruplex sequences are widely dispersed in eukaryotic genomes, including telomeres,[4] rDNA,[5] immunoglobulin switch regions,[6] and series of gene promoter regions, such as *c-myc*,[7] *c-kit*,[8] *bcl-2*,[9] and so on. G-Quadruplexes play important roles in many biological events. For example, the stable G-quadruplexes in telomeric DNA result in the inhibition of telomere elongation in cancer cells,[10,11] and the G-quadruplexes in many oncogene promoters function as a transcriptional repressor element.[12–17] Therefore, the binding and stabilization of the G-quadruplex by small molecule opens an opportunity for cancer therapeutics.

So far, some fused aromatic compounds, such as BRACO-19,[10,18] RHPS4,[19,20] MMQ1,[21] and SYUIQ-**5**[13] (Fig. 1a), and some unfused aromatic compounds, such as 1,4-triazole derivatives,[22] biarylpyrimidines,[23] triarylpyridines,[24] have been well characterized as G-quadruplex binding ligands. The common and the most favorable binding site for these ligands is the G-quartet surface.[25,26] Recently, from molecular dynamics (MD) simulation, we have suggested that fused aromatic ligand stacking on the G-quartet has a positive impact on G-quartet stabilization, and helps the overall G-quadruplex stabilization.[27] On the other hand, crystallographic or NMR structures of G-quadruplex have showed that the G-quartet surface is not completely coplanar.[28–31] MD studies have also suggested that the planarity of G-quartet surface is highly dynamics in solution.[27,32,33] Based on these considerations, unfused aromatic ligands with adaptive structural feature may be more suitable to be accommodated on the dynamic G-quartet surface rather than polycyclic compounds with rigid aromatic rings. Furthermore, this adaptive structural feature can prevent ligand from intercalating into the duplex DNA, and is consequently important for its strong quadruplex selectivity. However, in contrast to fused aromatic compounds, much less is known about how planarity of an unfused aromatic ligand influence its G-quadruplex binding properties.

Isaindigotone derivatives have been developed in our lab as selective telomeric G-quadruplex binding ligands.[11] The structure of a representative compound **SYUID-5a** is shown in Fig. 1b. Isaindigotone derivative has a unique asymmetric unfused

School of Pharmaceutical Sciences, Sun Yat-sen University, Guangzhou, 510006, People's Republic of China. E-mail: cesglq@mail.sysu.edu.cn, ceshzs@mail.sysu.edu.cn; Fax: 8620-39943056; Tel: 8620-39943056

† Electronic supplementary information (ESI) available. See DOI: 10.1039/c1ob05884c

 This journal is © The Royal Society of Chemistry 2011

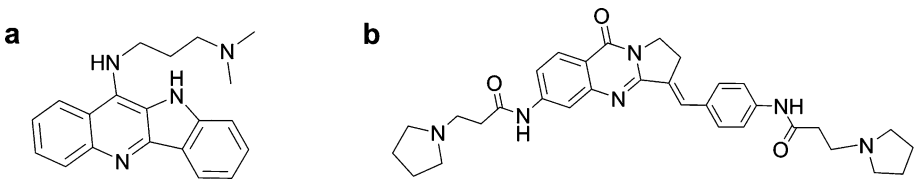

Fig. 1 Structures of **SYUIQ-5** (a) and **SYUID-5a** (b).

aromatic chromophore with an aliphatic five-member ring in the center core. Such a compound is neither polycyclic nor macrocyclic, and has free rotation around the single bond, which enables the adoption of possible twisted or coplanar conformations of the aryl groups. Our previous studies have suggested that these isaindigotone derivatives could occupy the G-quartet surface, and may also prevent ligand from intercalating into the duplex DNA.[11] Base on above studies, we perceive that isaindigotone derivatives offer an attractive template to investigate the influence of ligand planarity on the G-quadruplex binding properties. And a simple way to change the planarity of these molecules is to vary the aliphatic ring size which may also adjust the rotation of their benzylidene group. In the present study, isaindigotone derivatives with varying aliphatic ring size from five to seven were synthesized. Using telomeric G-quadruplex as a model, their interactions with this G-quadruplex were studied with FRET assay, SPR and CD. Molecular dynamics simulations were further carried out to elucidate this effect in detail.

Results and discussion

Design and syntheses of isaindigotone derivatives

To determine how the aliphatic ring affect the planar state of a molecule, the structures of compounds **SYUID-5a**, **7e** and **7h**, which have varied aliphatic ring size from five to seven, were constructed and optimized with GAUSSIAN using the HF/6-31G* basis set. As shown in Fig. 2, the nonplanarity of these compounds can be measured with the heights of their core region, which are best indicated from their side view. The heights for compounds **SYUID-5a**, **7e** and **7h** are 1.87, 2.41, and 3.65 Å, respectively. We can conclude that increasing the aliphatic ring size results in decreased planarity of their unfused aromatic core. To produce ligand diversity, a library of isaindigotone derivatives including 24 compounds was synthesized.

The isaindigotone derivatives were prepared following the procedure reported previously by our group.[11] The synthetic pathway for isaindigotone derivatives is shown in Scheme 1A and 1B. Compounds **2a–e** were synthesized from 2-amino-4-nitrobenzoic acid and 2-amino-5-nitrobenzoic acid in the presence of $POCl_3$. The reactions of compounds **2a–e** with 4-nitrobenzaldehyde or 4-dimethylaminobenzaldehyde through Claisen–Schmidt condensation yielded dinitro-compounds **3a–e**, and **5a–d**. Without further purification, these products were reduced to the corresponding diamino compounds **4a–e**, and **6a–d**. These products were assigned as *E* configuration on the basis of nuclear overhauser effect (NOE) analysis of NMR spectroscopy. In the NOE experiment, upon irradiation of proton 6-H and 6′-H, signals for protons 3-H and 4-H were simultaneously enhanced (as shown in the ESI†). Acylation of compounds **4a–e**, and **6a–d** were performed through their reactions with neat acid chloride. Their further amination was carried out with the required tertiary amine base (pyrrolidine/piperidine/dimethylamine) in the presence of ethanol to give desired target compounds.

FRET-melting studies

The stabilization of isaindigotone derivatives on telomeric G-quadruplex and duplex DNA was studied with FRET (fluorescence resonance energy transfer) based melting assay.[34–36] The isaindigotone derivative **SYUID-5a** and the quindoline derivative **SYUIQ-5** have been previously reported by us and were used as reference compounds in the present study.[11,37] Table 1 shows the effect of the ligand library on the enhanced melting temperature (ΔT_m) of two labeled oligonucleotides in solution containing K^+. F21T represents the human telomeric DNA, while F10T is a hairpin duplex DNA. Generally, the FRET-melting data showed that all of the derivatives could stabilize the telomeric G-quadruplex. Compounds **7a–7p** with double side chains were better quadruplex stabilizing ligands than compounds **7q–7x** with single side chain

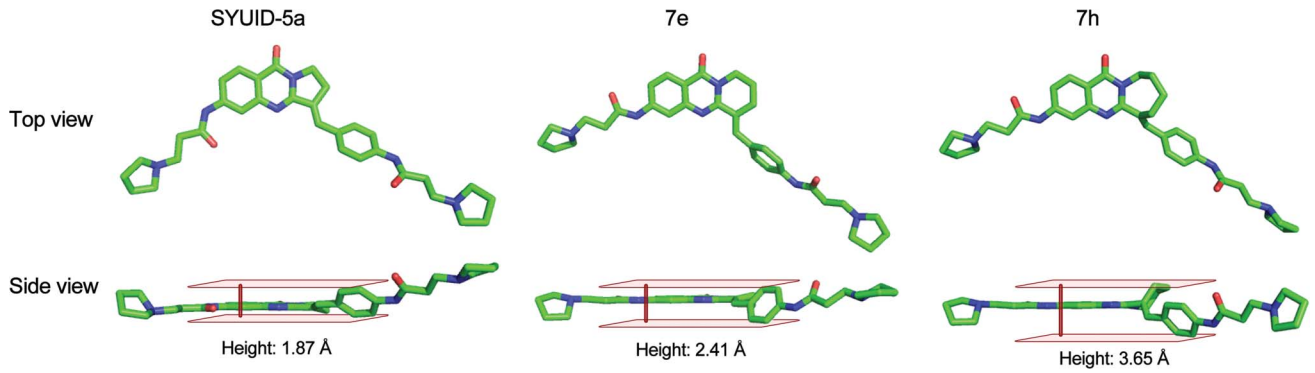

Fig. 2 Top view and side view of compounds **SYUID-5a**, **7e** and **7h**. The structure were calculated at the HF/6-31G* level.

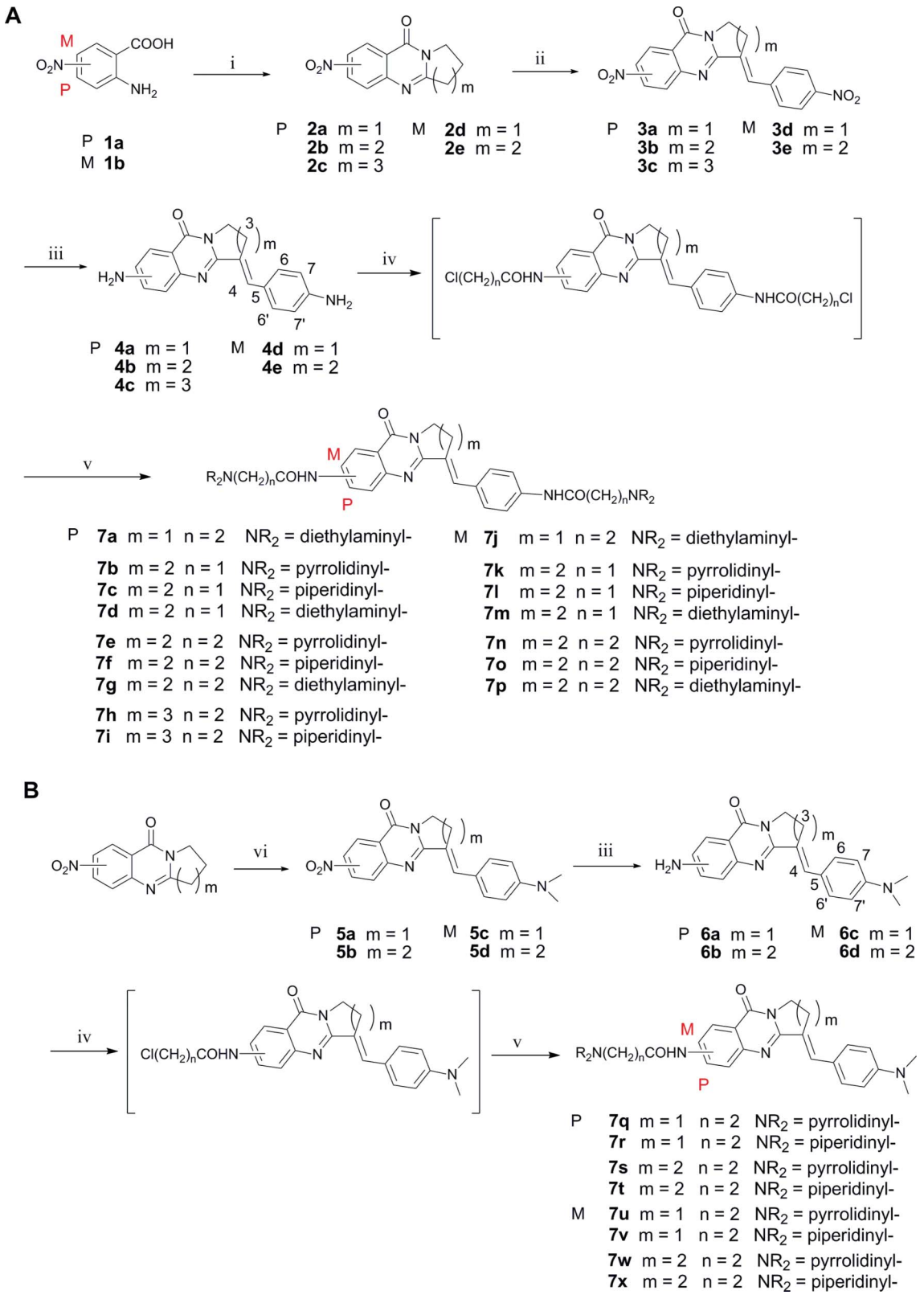

Scheme 1 Syntheses of isaindigotone derivatives. reagents: (i) pyrrolidin-2-one/piperidin-2-one/2- oxohexamethyleneimine, $POCl_3$, toluene (reflux); (ii) 4-nitrobenzaldehyde, Ac_2O (reflux); (iii) $Na_2S{\cdot}9H_2O$, NaOH, EtOH (reflux); (iv) $Cl(CH_2)_{n=1,2}COCl$ (reflux); (v) R_2NH, KI, ethanol (reflux); (vi) 4-dimethylaminobenzaldehyde, glacial acetic acid (reflux).

 This journal is © The Royal Society of Chemistry 2011

Table 1 Stabilization temperatures (ΔT_m) determined with FRET experiment[a]

Compound	F21T (ΔT_m/°C)	F10T (ΔT_m/°C)	Compound	F21T (ΔT_m/°C)	F10T (ΔT_m/°C)
7a	19.5 ± 1.7	1.1 ± 0.1	**7n**	9.0 ± 1.2	0.3 ± 0.1
7b	7.2 ± 0.8	0.3 ± 0.1	**7o**	8.5 ± 0.8	0.2 ± 0.2
7c	7.3 ± 0.7	0.3 ± 0.3	**7p**	8.2 ± 1.1	0.2 ± 0.2
7d	8.2 ± 0.9	0.4 ± 0.1	**7q**	4.1 ± 0.8	0.1 ± 0.2
7e	9.5 ± 1.2	0.6 ± 0.3	**7r**	4.4 ± 0.5	0.1 ± 0.2
7f	9.4 ± 0.9	0.4 ± 0.1	**7s**	2.0 ± 0.4	0.2 ± 0.0
7g	10.0 ± 1.5	0.2 ± 0.3	**7t**	2.0 ± 0.2	0.1 ± 0.2
7h	6.3 ± 0.7	0.3 ± 0.1	**7u**	2.6 ± 0.2	0.1 ± 0.1
7i	7.1 ± 0.6	0.2 ± 0.2	**7v**	3.2 ± 0.4	0.1 ± 0.0
7j	17.2 ± 1.8	0.6 ± 0.1	**7w**	1.3 ± 0.2	0.1 ± 0.0
7k	6.1 ± 0.6	0.3 ± 0.2	**7x**	1.2 ± 0.3	0.1 ± 0.0
7l	6.6 ± 0.8	0.2 ± 0.1	**SYUID-5a**	21.0 ± 1.1	0.7 ± 0.2
7m	6.5 ± 0.4	0.2 ± 0.0	**SYUIQ-5**	10.2 ± 0.2	5.1 ± 0.3

[a] $\Delta T_m = T_m$ (DNA + ligand) – T_m (DNA). The concentrations of F21T and F10T were both 0.2 μM. The concentrations of the compounds were 1μM. In the absence of ligand, T_m values of annealed F21T and F10T were 60 and 64 °C, respectively.

(Fig. 3A). For ligands **7a–7p** with double side chains, it was apparent that analogs **7a** and **7j** with five-member-ring were more effective quadruplex stabilizing ligands, with their ΔT_m values of 19.5 and 17.2 °C, respectively, while analogs **7e–g** and **7n–p** with six-member-ring were less effective quadruplex stabilizing ligands with their ΔT_m values in the range of 8.2–10.0 °C. The analogs **7h** and **7i** with seven-member-ring were the least effective quadruplex stabilizing ligands with their ΔT_m values of 6.3 and 7.1 °C, respectively. These results suggested that increasing aliphatic ring size resulted in a weaker quadruplex stabilizing effect. Such trend was consistent with their decreasing planarity.

It was also apparent that all compounds with P (*para* position)-substitution pattern, including compounds **7a–7g** and **7q–7t**, had generally an enhanced quadruplex stabilization compared to those with M (*meta* position)-substitution pattern including compounds **7j–7p** and **7u–7x**. In addition, the ΔT_m values for P-substituted isomers showed that the compounds with one methylene group (n = 1) on their side chain (**7b–d**) were slightly less effective in quadruplex stabilization than the compounds with two methylene groups (n = 2) on their side chain (**7e–g**). This trend was consistent with that for M-substituted isomers (**7k–m** and **7n–p**). Furthermore, no significant effect on ΔT_m values was observed if a pyrrolidinyl group was placed at the terminal of side chains instead of a piperidinyl or diethylaminyl group. The concentration dependent melting curves for ligands **7a,7e,7h,7j** and **7n** upon binding to F21T were showed in Fig. 3B.

The selectivity of these compounds for G-quadruplex over duplex DNA was also assessed by using FRET-based method. None of these compounds were found to significantly increase the melting temperature of FRET-tagged duplex DNA F10T (Table 1), suggesting their poor binding to the duplex DNA.[22,38] Furthermore, the G-quadruplex selectivity of some selected compounds

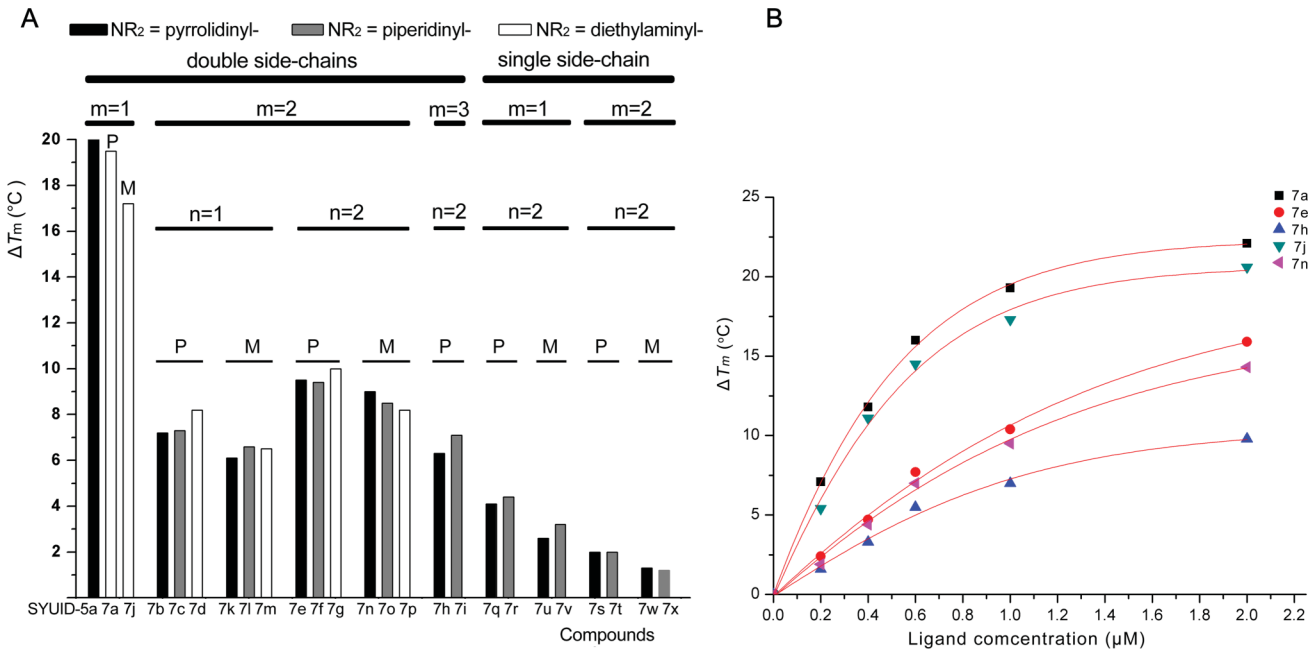

Fig. 3 (A) Stabilization temperatures of the isaindigotone derivatives. *m* represents the size of aliphatic ring, *n* represents the length of side chains, P and M represent *para* and *meta* position substitution, respectively. (B) Concentration dependent melting curves (ΔT_m *vs.* ligand concentration) for ligands **7a,7e,7h,7j** and **7n** upon binding to F21T.

Table 2 Kinetic parameters determined with SPR spectroscopy[a]

	SYUID-5a		7e		7h	
	Htelo[b]	Duplex[c]	Htelo[b]	Duplex[c]	Htelo[b]	Duplex[c]
k_a (M^{-1} s^{-1})	$1.53(\pm0.04)\times10^5$	—[d]	$3.87(\pm0.11)\times10^3$	—[d]	$3.08(\pm 0.12)\times10^2$	—[d]
k_d (s^{-1})	$2.70(\pm 0.03)\times10^{-2}$	—[d]	$2.05(\pm 0.02)\times10^{-3}$	—[d]	$1.67(\pm0.02)\times10^{-3}$	—[d]
K_D (M)	1.76×10^{-7}	—[d]	5.31×10^{-7}	—[d]	5.43×10^{-6}	—[d]
Chi^2	7.99		10.7		10.4	

[a] k_a is association constant, while k_d is dissociation constant. K_D denotes the equilibrium dissociation constant, given by k_d/k_a. The chi^2 value is a standard statistical measure of the closeness of fit. [b] Htelo (Quadruplex): 5-biotin-[$(GTTAGG)_5$]-3. [c] Duplex: 5-biotin-$T_9CGAATTCGT_5CGAATTCG$-3. [d] No significant binding was found for addition of up to 20 μM ligand.

was examined by using a FRET-based competition assay, and their activity in stabilizing G-quadruplex was challenged with nonfluorescent duplex DNA (ds26). In the presence of varying amount of competitor ds26, the thermal stabilization of F21T by the selected compounds was slightly affected (Fig. 4), while the stabilization of quadruplex by SYUIQ-5 was significantly decreased. The overall results of these assays demonstrated that isaindigotone derivatives could selectively bind to the quadruplex over duplex DNA, and an optimal G-quadruplex ligand should have a five-member-ring, P-substitution pattern, and double side chain.

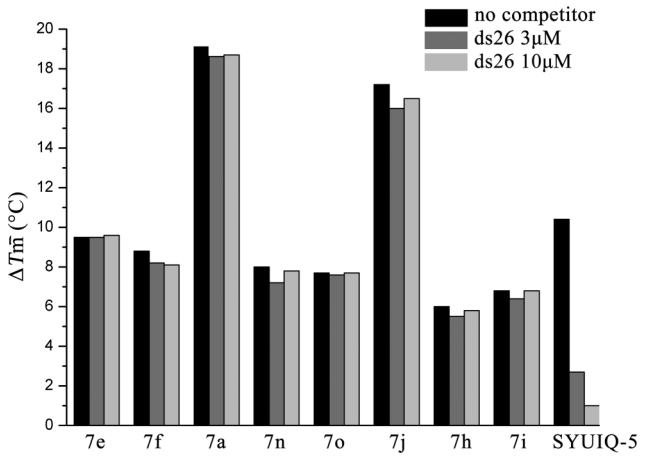

Fig. 4 Competitive FRET results for ligands **7a,7e–f**, **7j**, **7n–o**, **7h–i**, and **SYUIQ-5** (1 μM), without (black) and with 15-fold (3 μM; dark-gray) or 50-fold (10 μM; light-gray) excess of duplex DNA competitor (ds26). The concentration of F21T was 0.2 μM.

SPR assays

The kinetic constants of the compounds **SYUID-5a**, **7e**, and **7h** were assessed by surface plasmon resonance (SPR) against the human telomere and duplex DNA (Table 2, Fig S3). K_D was calculated by global fitting of the kinetic data from various concentrations of isaindigotone derivatives using 1 : 1 Langmuir binding. As showed in the Table 2, the binding affinity were in the order of **SYUID-5a** > **7e** > **7h**. This result suggested that increasing aliphatic ring size decreases the planarity of the compounds, and consequently resulted in a decrease of their quadruplex binding affinity. This result is consistent with that from the above FRET studies. These compounds exhibited good G-quadruplex/duplex DNA selectivity, with no duplex DNA interaction detected under the experimental conditions used.

CD studies

Circular dichroism (CD) spectroscopy was used to study the binding property of the isaindigotone derivatives to telomeric G-quadruplex.[39] In the absence of salt, the CD spectrum of the human telomeric sequence $d[G_3(T_2AG_3)_3]$ (HTG21) was found to exhibit a negative band at 238 nm, a major positive band at 255 nm, a minor negative band at 278 nm, and a positive band at 295 nm (Fig. 5A).[40] Upon addition of excess compound **SYUID-5a**

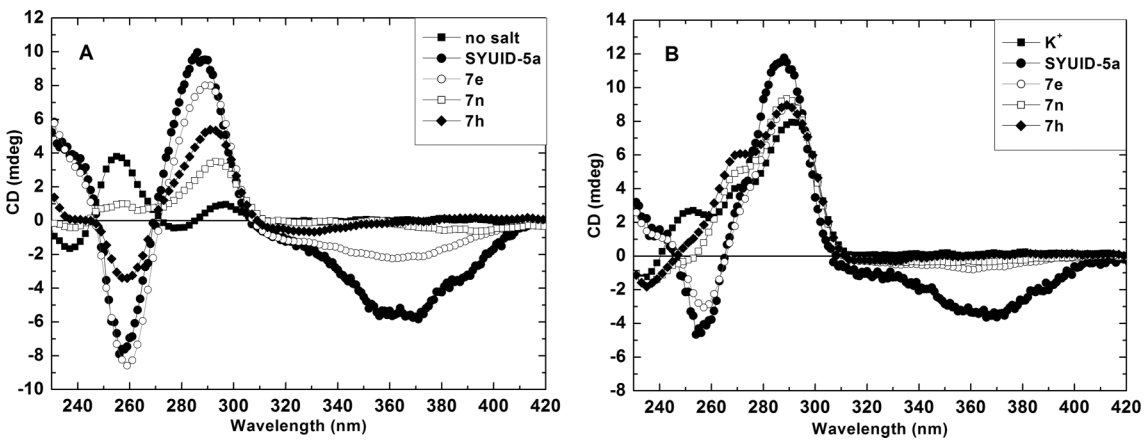

Fig. 5 (A) CD spectra of 5 μM HTG21 in 10 mM Tris–HCl buffer, pH 7.2, without cations and drug (■), with 20 μM compound **SYUID-5a** (●), 20 μM compound **7e** (○), 20 μM compound **7n** (□), and 20 μM compound **7h** (◆). (B) CD spectra of 5 μM HTG21 in 10 mM Tris–HCl buffer, pH 7.2, with 150 mM K^+ (■), 20 μM compound **SYUID-5a** (●), 20 μM compound **7e** (○), 20 μM compound **7n** (□), and 20 μM compound **7h** (◆).

 This journal is © The Royal Society of Chemistry 2011

(4 mol equiv) to the HTG21, a dramatic change in the CD spectra was observed. The bands at 238, 255, and 278 nm disappeared and a major negative band at 258 nm appeared, while the band centered at 292 nm significantly increased and shifted toward 286 nm. These changes suggested that the G-rich DNA HTG21 was induced by compound **SYUID-5a** to form G-quadruplex structure. In addition, the strong and negative induced CD signal around 360 nm was additional evidence for the interaction between the G-quadruplex and **SYUID-5a** because its appearance in the CD spectra is indicative of an achiral ligand binding tightly to a chiral host.[41] The CD spectra of the HTG21 oligonucleotide for the addition of compound **7e** and **7h** in the absence of salt were similar to that for the addition of compound **SYUID-5a**. However, the band intensity for compound **7h** was weaker than that of compound **SYUID-5a** and **7e**. This result indicated that compound **7h** was less effective in induction of G-quadruplex formation than compound **SYUID-5a** and **7e**. In addition, upon addition of compound **7n** to the HTG21 oligonucleotide, slight changes were observed in the CD spectra, where a band centered at 295 nm increased and a band at 255 nm decreased without obvious band shift. These results indicated that compound **7n** could also induce the telomeric G-rich DNA to form the G-quadruplex structure, but the ligand was much less effective in initiating the topological change of G-rich DNA compared to compound **7e** and **7h**. Overall, these results suggested that increasing the size of aliphatic ring had a negative impact on the ability of ligands in inducing quadruplex formation. The ligands with P-substitution were more effective in inducing G-quadruplex formation than the ligands with M-substitution. These results are consistent with those from FRET and SPR studies.

It has been reported that HTG21 oligonucleotide has formed the hybrid-type G-quadruplex structure in the presence of K^+, with a large positive band at 290 nm, a small positive band at 265 nm, and a negative band at 235 nm (Fig. 5B).[29,42] Upon our titration of this DNA solution with compound **SYUID-5a**, the band at 265 nm disappeared, while the band at 257 nm appeared. An additional induced CD signal around 360 nm was also observed. The CD spectrum of G-quadruplex for the titration with compound **7e** was similar to that with compound **SYUID-5a**. However, upon the addition of compound **7h** and **7n** into the solution of hybrid G-quadruplex with K^+, no significant change was observed in the resulting CD spectra.

NMR studies and molecular modeling

To further investigate the binding modes between the isaindigotone derivatives and G-quadruplex structures, nuclear magnetic resonance (NMR) studies and molecular modeling studies were performed. The intermolecular four-stranded parallel quadruplex [$d(T_2AG_3)$] derived from human telomeric DNA sequences was used in this study.[43] NMR titration experiments showed most ^1H NMR signals exhibited progressive shifts and line broadening at increasing ligand concentration (Fig S4). This effect was slightly more apparent for imino proton signals of G4 in all complexes. Furthermore, the A3H2, A3H8, and G4H8 imino proton signals exhibited significant line broadening at increasing ligand concentration. These results suggested that the studied ligands preferred to stack between the A3 and G4 residues. In addition, the changes of ^1H NMR signals were more significant for **SYUID-5a**-quadruplex complex rather than **7e**-quadruplex complex and **7h**-quadruplex complex. This result is consistent with those from the above studies. Decreasing ligands' planarity resulted in their decreased interactions with quadruplex.

Molecular docking and molecular dynamics simulations were carried out in order to understand the nature of the ligand–DNA interactions, and help rationalize the experimental result.[44] Molecular docking studies were used to predict the possible interactions between the ligands and G-quadruplex DNA. The NMR-determined mixed hybrid-type G-quadruplex structure (PDB 2HY9)[45] was used as the template for the modeling studies because it might be a more relevant form in the presence of K^+ ion in dilute solution.[46] Our previous studies have shown that compound **SYUID-5a** bound to the telomeric quadruplex *via* multiple binding modes. Besides the end-stacking mode, groove binding mode has also been possible. However, the end-stacking mode has shown higher binding energy than that of groove binding mode from MM-PBSA calculations, and G-quartet might be the major binding site for the increased stability of G-quadruplex.[11,27] Hence, the modeling of end-stacking interaction can help rationalize the FRET and SPR results. In the present study, we only focused on the end-stacking binding mode. One hundred docking conformers of ligand-quadruplex complexes from molecular docking studies showed that ligands predominantly stacked on the 5′ end of the G-quadruplex (Fig. S5). Therefore, the most probable conformation of each ligand on 5′ end was chosen, which showed a good stacking arrangement with the G-tetrads. On the basis of the docking results, MD simulations (10 ns) were performed on two complexes formed by hybrid-type G-quadruplexes with ligand **7e** and **7h** (MD simulation of **SYUID-5a**-quadruplex complex has been reported by our group[11]). Both models were quite stable during the dynamics runs (Fig. S6). The complexes formed by G-quadruplex with **7e** and **7h** are shown in Fig. 6. These two ligands bound to the G-quartet in a very similar pattern. The unfused aromatic rings that form the central pharmacophore stacked over the guanine tetrads with maximized π–π stacking interactions. The presence of the tertiary amine at the ends of the side chains contributed to stabilization of the G-quadruplex by forming hydrogen bonds to phosphate groups. The terminal tertiary amine is usually protonated at physiological pH, and the presence of positive charge would enhance its electrostatic interactions with the negatively charged atoms of the loops.

To study the heat stability of the G-quartet after ligand binding, we elongated the simulation time for another 2 ns at 350 K. The hydrogen bond (N1–H···N7 and N2–H···O6) occupancies of the G-quartet were calculated as shown in Fig. 7. An interaction was considered to be a hydrogen bond if the distance between the hydrogen donor and acceptor was less than 3.5 Å, and the binding angle was greater than 120.0°. The Hoogsteen hydrogen bonds in a G-quadruplex are the main forces for keeping quartets stable. The **SYUID-5a**-quadruplex complex has the highest average hydrogen bond occupancy (98.56%), the next is **7e**-quadruplex complex (98.45%), and the remaining is **7h**-quadruplex complex (97.83%). These results are consistent with those from FRET studies, which suggested that a larger aliphatic ring size resulted in a weaker G-quadruplex stabilization effect.

Besides, the binding free energy was further calculated with MM-PBSA method. Table 3 shows all of the energy terms given for each compound. According to Table 3, the calculated binding

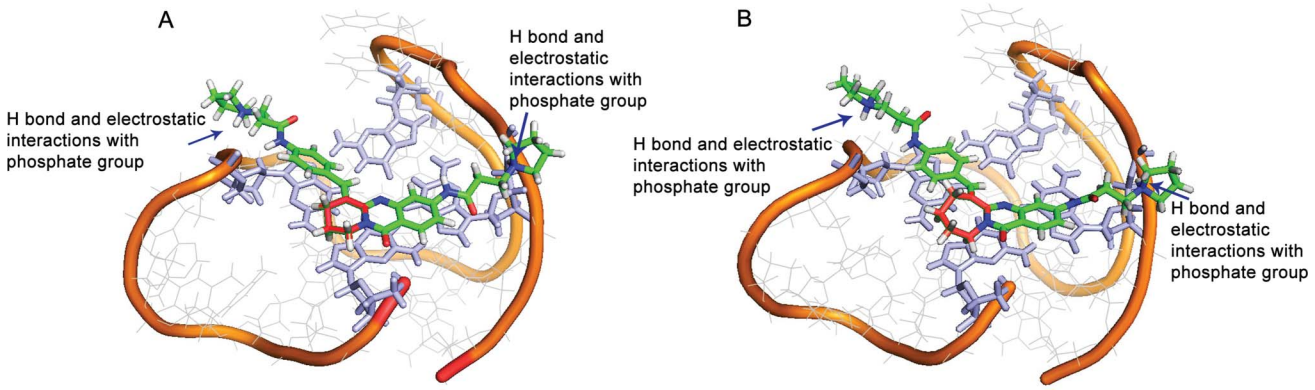

Fig. 6 Averaged structures obtained by averaging 50 MD simulation snapshots from the last 2 ns on the MD trajectory with an interval of 20 ps. (A) **7e**-quadruplex complex; (B) **7h**-quadruplex complex. Pictures were generated by PYMOL.[47]

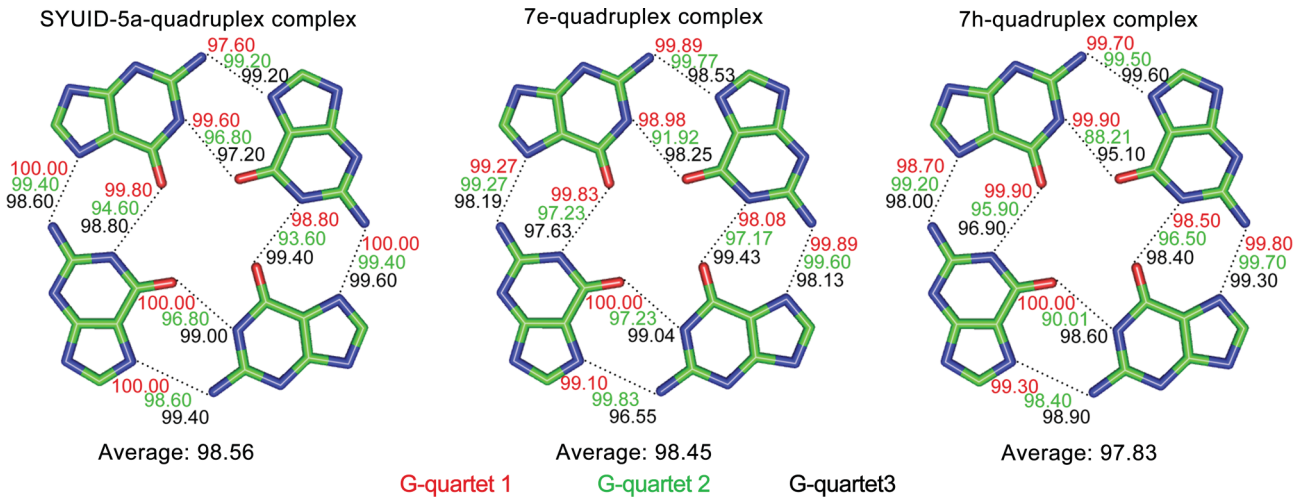

Fig. 7 Hydrogen bond occupancies within every G-quartet during MD simulations at 350 K. Occupancy is provided as a percentage of the investigated time period.

Table 3 Energetic analysis of ligand-quadruplex complex formations (kcal mol^{-1})[a]

Compound	ΔE_{elec}	ΔE_{vdw}	ΔG_{np}	ΔG_{PB}	ΔG_{tot}	$-T\Delta S$	ΔG_{bind}
SYUID-5a	–913.84	–54.94	–6.60	926.98	–48.41	27.14	–21.27
7e	–924.59	–54.16	–6.01	936.15	–48.60	29.88	–18.12
7h	–849.18	–49.75	–5.64	861.69	–42.88	28.46	–14.42

[a] ΔE_{elec} is the electrostatic molecular-mechanical energy. ΔE_{vdw} is the van der Waals molecular-mechanical energy. ΔG_{np} is the nonpolar contribution to the solvation energy. ΔG_{PB} is the electrostatic contribution to the solvation energy calculated by the PB approach. ΔG_{tot} is the total energy without solute entropic contribution ($\Delta E_{elec} + \Delta E_{vdw} + \Delta G_{np} + \Delta G_{PB}$). $-T\Delta S$ is the solute entropic contribution, where T = temperature and S = sum of translational, rotational, and vibrational entropy. ΔG_{bind} is the total energy with solute entropic contribution ($\Delta G_{tot} - T\Delta S$).

free energy (ΔG_{bind}) for ligands was in agreement with the results from SPR studies. A detailed analysis suggested that, van der Waals (ΔE_{vdw}) and electrostatic energy (ΔE_{elec}) had major favorable contribution to the binding, while polar solvation energy (ΔG_{PB}) and entropic effect ($-T\Delta S$) were unfavorable for the binding. On the other hand, nonpolar solvation energy (ΔG_{np}) had slightly favorable contribution. However, the favorable electrostatic energy was counteracted by the unfavorable polar solvation energy, and as a result, the van der Waals energy and the entropic effect became the major factors. The van der Waals energy for compounds **SYUID-5a** and **7e** was very similar, while that for compound **7h** was ~5 kcal mol^{-1} higher. This result suggested that both compound **7e** and **SYUID-5a** stacked on the G-quartet surface well. However, the seven member aliphatic ring in the central pharmacophore of compound **7h** would interfere with its stacking interaction with G-quartet surface, thus leading to decreased binding affinity.

To further investigate the structural feature of compounds that impact on the G-quadruplex binding properties in detail, the distance deviations between the quinazoline motifs and G-quartet surface were calculated (Fig. 8). As shown in Fig. 8B, the distance deviation was in the order of **SYUID-5a**-quadruplex complex > **7e**-quadruplex complex > **7h**-quadruplex complex. The average distances between the quinazoline motifs and G-quartet surface

 This journal is © The Royal Society of Chemistry 2011

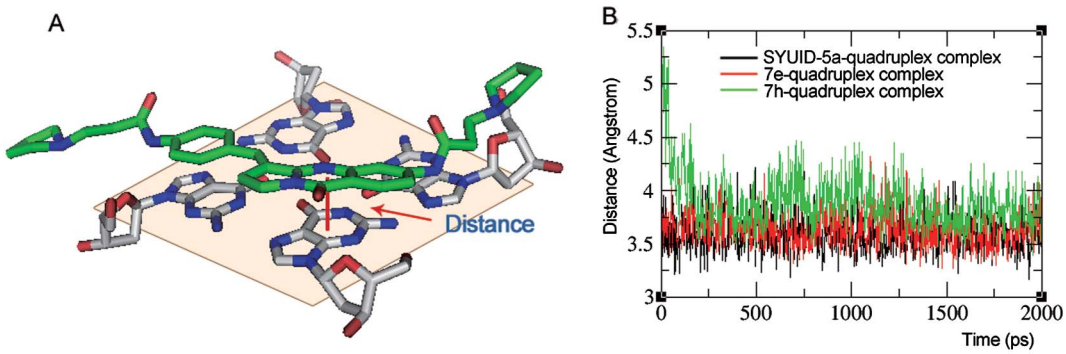

Fig. 8 (A) Distance between the quinazoline motifs and G-quartet surface. (B) Distance deviations between the quinazoline motifs and G-quartet surface calculated from the last 2 ns trajectories.

were 3.59 Å, 3.63 Å, and 3.89 Å for **SYUID-5a**-quadruplex, **7e**-quadruplex, and **7h**-quadruplex complex, respectively. This result indicated that **SYUID-5a** stabilized G-quadruplex better than **7e**, and **7e** did better than **7h**. Due to the steric clashes between their unfused aromatic core and G-quartet surface, increasing the aliphatic ring size resulted in increased distance between the quinazoline motifs and G-quartet surface. This result again supported the experimental observation that increasing the aliphatic ring size resulted in decreased stacking interaction with G-quartet.

Conclusion

A series of isaindigotone derivatives as telomeric quadruplex ligands were designed, synthesized and characterized by using CD spectroscopy, FRET-melting assay, and SPR. NMR studies suggested that these compounds could stack over the G-quartet surface. Through changing the aliphatic ring size in the middle core of these ligands, the planarity of main core was adjusted in three levels. The decreased planarity resulted in their decreased binding affinity and stabilization ability. Molecular modeling studies confirmed our hypothesis that the aliphatic ring in a ligand molecule was the key structural basis responsible for this effect. Comparing to the fused aromatic ligands with rigid core, the unfused aromatic ligands are flexible and more suitable to be accommodated on the dynamic G-quartet surface. However, there are flexibility limitations for the ligands to achieve both optimal binding affinity and optimal binding selectivity for G-quadruplex. In fact, for isaindigotone derivatives, more planar compounds have generally stronger G-quadruplex binding affinity and stabilization ability. This study provided insight information about how quadruplex binding affinity and selectivity could be adjusted by controlling the planarity of a ligand, which shed light on further development of isaindigotone derivatives for selective and potent G-quadruplex binding ligands.

Experimental section

Synthesis and characterization

All chemicals were obtained from commercial sources unless otherwise specified. ^{1}H NMR, ^{13}C NMR and NOESY spectra were recorded using TMS as the internal standard in DMSO-*d6* or $CDCl_3$ with a Bruker BioSpin GmbH spectrometer at 400.132, 100.614 and 400.132 MHz, respectively. Mass spectra (MS) were recorded on a Shimadzu LCMS-2010A instrument with an ESI or ACPI mass selective detector, and high resolution mass spectra (HRMS) on Shimadzu LCMS-IT-TOF. Melting points (mp) were determined using a SRS-OptiMelt automated melting point instrument without correction.

3-Nitro-8,9-dihydro-6*H*-pyrido[2,1-*b*]quinazolin-11(7*H*)-one (2b). To a stirred suspension of piperidin-2-one (0.50 g, 5 mmol) and 2-amino-4-nitrobenzoic acid (1.8 g, 10 mmol) in 250 mL anhydrous toluene, $POCl_3$ (3 mL) was added dropwise at room temperature, and the mixture was heated under reflux for 8 h. The reaction product was poured onto ice, and then concentrated ammonium hydroxide was added to make the solution basic. The precipitate was separated from water through filtration, and the filtrate was extracted with 3 × 100 mL of ethyl acetate. The combined organic phase was washed with 100 mL of water containing 10 mL of concentrated ammonium hydroxide, dried over magnesium sulfate, and concentrated to dryness. The resulting residue combined with previous precipitate was purified using flash chromatography with cyclohexane/ethyl acetate elution to afford compound **2b** as a pale-yellow solid with a yield of 37%. Mp: 180–182 °C. ^{1}H NMR (400 MHz, $CDCl_3$) δ 8.44 (d, J = 2.1 Hz, 1H), 8.41 (d, J = 8.8 Hz, 1H), 8.17 (dd, J = 8.8, 2.1 Hz, 1H), 4.10 (t, J = 6.2 Hz, 2H), 3.05 (t, J = 6.6 Hz, 2H), 2.10 – 1.95 (m, 4H). ESI-MS m/z calcd $C_{12}H_{11}N_3O_3$ $[M + H]^+$ 246.1, found 246.1.

3-Nitro-7,8,9,10-tetrahydroazepino[2,1-*b*]quinazolin-12(6*H*)-one (2c). The method for the preparation of compound **2b** was used except replacing piperidin-2-one with 2-oxohexamethyleneimine. Compound **2c** was synthesized as a pale-yellow solid with a yield of 25%. Mp: 147–150 °C. ^{1}H NMR (400 MHz, $CDCl_3$) δ 8.41 (d, J = 2.1 Hz, 1H), 8.38 (d, J = 8.8 Hz, 1H), 8.16 (dd, J = 8.8, 2.1 Hz, 1H), 4.46 – 4.36 (m, 2H), 3.17 – 3.07 (m, 2H), 1.97 – 1.80 (m, 6H). ESI-MS m/z calcd $C_{13}H_{13}N_3O_3$ $[M + H]^+$ 260.1, found 260.1.

2-Nitro-8,9-dihydro-6*H*-pyrido[2,1-*b*]quinazolin-11(7*H*)-one (2e). The method for the preparation of compound **2b** was used except replacing 2-amino-4-nitrobenzoic acid with 2-amino-5-nitrobenzoic acid. Compound **2e** was synthesized as a pale-yellow solid with a yield of 50%. Mp: 182–183 °C. ^{1}H NMR (400 MHz, $CDCl_3$) δ 9.13 (d, J = 2.6 Hz, 1H), 8.50 (dd, J = 9.0, 2.6 Hz, 1H), 7.71 (d, J = 9.0 Hz, 1H), 4.11 (t, J = 6.2 Hz, 2H), 3.06 (t,

J = 6.6 Hz, 2H), 2.09–1.96 (m, 4H). ESI-MS m/z calcd $C_{12}H_{11}N_3O_3$ $[M + H]^+$ 246.1, found 246.1.

(*E*)-3-Nitro-6-(4-nitrobenzylidene)-8,9-dihydro-6*H*-pyrido[2,1-*b*]quinazolin-11(7*H*)-one (3b). A mixture of compound **2b** (1.2 g, 5.0 mmol), 4-nitrobenzaldehyde or 4-dimethylaminobenzaldehyde (10 mmol), and NaOAc (0.082 g, 1.0 mmol) in glacial acetic acid (10 mL) was heated under reflux for 8 h. After cooling to room temperature, the precipitate was separated from solvent through filtration and rinsed with chloroform (100 mL) and acetone (200 mL) to afford compound **3b** as a pale-yellow solid with a yield of 93%. Mp: 276–278 °C. ^{1}H NMR (400 MHz, DMSO) δ 8.45 (d, J = 2.1 Hz, 1H), 8.41–8.26 (m, 4H), 8.22 (dd, J = 8.8, 2.1 Hz, 1H), 7.85 (d, J = 8.7 Hz, 2H), 4.15–4.04 (m, 2H), 3.00–2.88 (m, 2H), 2.07–1.94 (m, 2H). ESI-MS m/z calcd $C_{19}H_{14}N_4O_5$ $[M + H]^+$ 379.1, found 379.1.

(*E*)-3-Nitro-6-(4-nitrobenzylidene)-7,8,9,10-tetrahydroazepino-[2,1-*b*]quinazolin-12(6*H*)-one (3c). The method for the preparation of compound **3b** was used, with compound **2c** as starting material. Compound **3c** was synthesized as a pale-yellow solid with a yield of 42%. Mp: 250–253 °C. ^{1}H NMR (400 MHz, $CDCl_3$) δ 8.60 (d, J = 2.1 Hz, 1H), 8.47 (d, J = 8.7 Hz, 1H), 8.30 (d, J = 8.7 Hz, 2H), 8.26 (dd, J = 8.7, 2.1 Hz, 1H), 7.67 (d, J = 8.7 Hz, 2H), 7.23 (s, 1H), 4.38–4.30 (m, 2H), 2.87–2.79 (m, 2H), 2.03–1.90 (m, 4H). ESI-MS m/z calcd $C_{20}H_{16}N_4O_5$ $[M + H]^+$ 393.1, found 393.1.

(*E*)-2-Nitro-6-(4-nitrobenzylidene)-8,9-dihydro-6*H*-pyrido[2,1-*b*]quinazolin-11(7*H*)-one (3e). The method for the preparation of compound **3b** was used, with compound **2e** as starting material. Compound **3e** was synthesized as a pale-yellow solid with a yield of 93%. Mp: 244–247 °C. ^{1}H NMR (400 MHz, DMSO) δ 8.84 (d, J = 2.4 Hz, 1H), 8.56 (dd, J = 9.0, 2.4 Hz, 1H), 8.37 (s, 1H), 8.31 (d, J = 8.7 Hz, 2H), 7.90 (d, J = 9.0 Hz, 1H), 7.85 (d, J = 8.7 Hz, 2H), 4.13–4.05 (m, 2H), 2.98–2.91 (m, 2H), 2.04–1.96 (m, 2H). ESI-MS m/z calcd $C_{19}H_{14}N_4O_5$ $[M + H]^+$ 379.1, found 379.1.

(*E*)-3-(4-(Dimethylamino)benzylidene)-6-nitro-2,3-dihydropyrrolo[2,1-*b*]quinazolin-9(1*H*)-one (5a). The method for the preparation of compound **3b** was used. Compound **2a** was reacted with 4-dimethylaminobenzaldehyde to afford compound **5a** as a red solid with a yield of 82%. Mp: 271–272 °C. ^{1}H NMR (400 MHz, $CDCl_3$) δ 8.52 (d, J = 2.1 Hz, 1H), 8.38 (d, J = 8.7 Hz, 1H), 8.10 (dd, J = 8.7, 2.1 Hz, 1H), 7.81 (s, 1H), 7.48 (d, J = 8.7 Hz, 2H), 6.73 (d, J = 8.7 Hz, 2H), 4.34–4.23 (m, 2H), 3.34–3.23 (m, 2H), 3.05 (s, 6H). ESI-MS m/z calcd $C_{20}H_{18}N_4O_5$ $[M + H]^+$ 363.1, found 363.1.

(*E*)-6-(4-(Dimethylamino)benzylidene)-3-nitro-8,9-dihydro-6*H*-pyrido[2,1-*b*]quinazolin-11(7*H*)-one (5b). The method for the preparation of compound **3b** was used except replacing 4-nitrobenzaldehyde with 4-dimethylaminobenzaldehyde. Compound **5b** was synthesized as a red solid with a yield of 78%. Mp: 206–209 °C. ^{1}H NMR (400 MHz, $CDCl_3$) δ 8.43 (d, J = 2.1 Hz, 1H), 8.29 (d, J = 8.7 Hz, 1H), 8.17 (s, 1H), 8.01 (dd, J = 8.7, 2.1 Hz, 1H), 7.40 (d, J = 8.8 Hz, 2H), 6.66 (d, J = 8.8 Hz, 2H), 4.14–4.02 (m, 2H), 2.97 (s, 6H), 2.95–2.89 (m, 2H), 2.02–1.93 (m, 2H). ESI-MS m/z calcd $C_{21}H_{20}N_4O_3$ $[M + H]^+$ 377.2, found 377.2.

(*E*)-3-(4-(Dimethylamino)benzylidene)-7-nitro-2,3-dihydropyrrolo[2,1-*b*]quinazolin-9(1*H*)-one (5c). The method for the preparation of compound **3b** was used. Compound **2d** was reacted with 4-dimethylaminobenzaldehyde to afford compound **5c** as a red solid with a yield of 81%. Mp: 287–290 °C. ^{1}H NMR (400 MHz, $CDCl_3$) δ 9.11 (d, J = 2.0 Hz, 1H), 8.48 (d, J = 9.0 Hz, 1H), 7.87 (s, 1H), 7.77 (d, J = 9.0 Hz, 1H), 7.50 (d, J = 8.8 Hz, 2H), 6.75 (d, J = 8.8 Hz, 2H), 4.38–4.30 (m, 2H), 3.35–3.27 (m, 2H), 3.08 (s, 6H). ESI-MS m/z calcd $C_{20}H_{18}N_4O_3$ $[M + H]^+$ 363.1, found 363.2.

(*E*)-6-(4-(Dimethylamino)benzylidene)-2-nitro-8,9-dihydro-6*H*-pyrido[2,1-*b*]quinazolin-11(7*H*)-one (5d). The method for the preparation of compound **3b** was used. Compound **2e** was reacted with 4-dimethylaminobenzaldehyde to afford compound **5d** as a red solid with a yield of 82%. Mp: 206–208 °C. ^{1}H NMR (400 MHz, $CDCl_3$) δ 9.05 (d, J = 2.6 Hz, 1H), 8.40 (dd, J = 9.0, 2.6 Hz, 1H), 8.25 (s, 1H), 7.67 (d, J = 9.0 Hz, 1H), 7.42 (d, J = 8.8 Hz, 2H), 6.67 (d, J = 8.8 Hz, 2H), 4.14–4.08 (m, 2H), 2.99 (s, 6H), 2.97–2.91 (m, J = 5.7 Hz, 2H), 2.04–1.95 (m, 2H). ESI-MS m/z calcd $C_{21}H_{20}N_4O_3$ $[M + H]^+$ 377.2, found 377.1.

(*E*)-3-Amino-6-(4-aminobenzylidene)-8,9-dihydro-6*H*-pyrido[2,1-*b*]quinazolin-11(7*H*)-one (4b). To a stirred suspension of compound **3b** (1.9 g, 5.0 mmol) in ethanol (50 mL) was added a solution of $Na_2S{\cdot}9H_2O$ (4.8 g, 20 mmol) and NaOH (2 g, 50 mmol) in water (80 mL). The mixture was heated under reflux for 6 h. The ethanol was removed *in vacuo*, and the residue was cooled to 0–5 °C. The resulting precipitate was collected through filtration, repeatedly washed with water, and dried to afford compound **4b** as an orange–red solid with a yield of 91%. Mp: 230–232 °C. ^{1}H NMR (400 MHz, DMSO) δ 7.91 (s, 1H), 7.73 (d, J = 8.6 Hz, 1H), 7.27 (d, J = 8.5 Hz, 2H), 6.65 (dd, J = 8.6, 2.1 Hz, 1H), 6.61 (d, J = 8.5 Hz, 2H), 6.60–6.57 (m, 1H), 5.96 (s, 2H), 5.57 (s, 2H), 4.00–3.90 (m, 2H), 2.87–2.78 (m, 2H), 1.93–1.83 (m, 2H). ESI-MS m/z calcd $C_{19}H_{18}N_4O$ $[M + H]^+$ 319.2, found 319.2.

(*E*)-3-Amino-6-(4-aminobenzylidene)-7,8,9,10-tetrahydroazepino[2,1-*b*]quinazolin-12(6*H*)-one (4c). The method for the preparation of compound **4b** was used, with compound **3c** as starting material. Compound **4c** was synthesized as an orange–red solid with a yield of 61%. Mp: 240–241 °C. ^{1}H NMR (400 MHz, DMSO) δ 7.76 (d, J = 8.6 Hz, 1H), 7.25 (d, J = 8.6 Hz, 2H), 6.79 (s, 1H), 6.70 (dd, J = 8.6, 2.2 Hz, 1H), 6.64–6.59 (m, 3H), 6.03 (s, 2H), 5.44 (s, 2H), 4.09–4.03 (m, 2H), 2.70–2.64 (m, 2H), 1.80–1.67 (m, 4H). ESI-MS m/z calcd $C_{20}H_{20}N_4O$ $[M + H]^+$ 333.2, found 333.2.

(*E*)-2-Amino-6-(4-aminobenzylidene)-8,9-dihydro-6*H*-pyrido[2,1-*b*]quinazolin-11(7*H*)-one (4e). The method for the preparation of compound **4b** was used, with compound **3e** as starting material. Compound **4e** was synthesized as an orange–red solid with a yield of 90%. Mp: 207–209 °C. ^{1}H NMR (400 MHz, DMSO) δ 7.83 (d, J = 2.0 Hz, 1H), 7.38 (d, J = 8.7 Hz, 1H), 7.24 (d, J = 8.5 Hz, 2H), 7.18 (s, 1H), 7.07 (dd, J = 8.7, 2.0 Hz, 1H), 6.61 (d, J = 8.5 Hz, 2H), 5.55 (s, 2H), 5.51 (s, 2H), 4.05–3.95 (m, 2H), 2.87–2.79 (m, 2H), 1.94–1.84 (m, 2H). ESI-MS m/z calcd $C_{19}H_{18}N_4O$ $[M + H]^+$ 319.2, found 319.2.

(*E*)-6-Amino-3-(4-(dimethylamino)benzylidene)-2,3-dihydropyrrolo[2,1-*b*]quinazolin-9(1*H*)-one (6a). The method for the preparation of compound **4b** was used, with compound **5a** as starting material. Compound **6a** was synthesized as an orange–red solid with a yield of 92%. Mp: 256–258 °C. ^{1}H NMR (400 MHz, DMSO) δ 7.77 (d, J = 8.5 Hz, 1H), 7.54 (s, 1H), 7.47 (d, J = 8.8 Hz, 2H), 6.77 (d, J = 8.7 Hz, 2H), 6.69–6.63 (m, 2H), 6.01 (s, 2H),

 This journal is © The Royal Society of Chemistry 2011

4.08–4.03 (m, 2H), 3.17–3.10 (m, 2H), 2.97 (s, 6H). ESI-MS *m/z* calcd $C_{20}H_{20}N_4O$ [M + H]$^+$ 333.2, found 333.1.

(*E*)-3-Amino-6-(4-(dimethylamino)benzylidene)-8,9-dihydro-6*H*-pyrido[2,1-*b*]quinazolin-11(7*H*)-one (6b). The method for the preparation of compound **4b** was used, with compound **5b** as starting material. Compound **6b** was synthesized as an orange–red solid with a yield of 86%. Mp: 196–197 °C. ^{1}H NMR (400 MHz, DMSO) δ 7.96 (s, 1H), 7.75 (d, J = 8.8 Hz, 1H), 7.41 (d, J = 8.6 Hz, 2H), 6.74 (d, J = 8.6 Hz, 2H), 6.67 (d, J = 8.8 Hz, 1H), 6.62 (s, 1H), 6.02 (s, 2H), 4.02–3.89 (m, 2H), 2.94 (s, 6H), 2.90–2.80 (m, 2H), 1.96–1.82 (m, 2H). ESI-MS *m/z* calcd $C_{21}H_{22}N_4O$ [M + H]$^+$ 347.2, found 347.2.

(*E*)-7-Amino-3-(4-(dimethylamino)benzylidene)-2,3-dihydropyrrolo[2,1-*b*]quinazolin-9(1*H*)-one (6c). The method for the preparation of compound **4b** was used, with compound **5c** as starting material. Compound **6c** was synthesized as an orange–red solid with a yield of 81%. Mp: 249–253 °C. ^{1}H NMR (400 MHz, DMSO) δ 7.48–7.43 (m, 3H), 7.41 (d, J = 8.7 Hz, 1H), 7.22 (d, J = 2.5 Hz, 1H), 7.07 (dd, J = 8.7, 2.5 Hz, 1H), 6.76 (d, J = 8.7 Hz, 2H), 5.59 (s, 2H), 4.10 (t, J = 7.2 Hz, 2H), 3.15 (t, J = 6.3 Hz, 2H), 2.96 (s, 6H). ESI-MS *m/z* calcd $C_{20}H_{20}N_4O$ [M + H]$^+$ 333.2, found 333.1.

(*E*)-2-Amino-6-(4-(dimethylamino)benzylidene)-8,9-dihydro-6*H*-pyrido[2,1-*b*]quinazolin-11(7*H*)-one (6d). The method for the preparation of compound **4b** was used, with compound **5d** as starting material. Compound **6d** was synthesized as an orange–red solid with a yield of 79%. Mp: 244–246 °C. ^{1}H NMR (400 MHz, $CDCl_3$) δ 8.01 (s, 1H), 7.57 (d, J = 8.7 Hz, 1H), 7.47–7.40 (m, 3H), 7.10 (dd, J = 8.7, 2.8 Hz, 1H), 6.73 (d, J = 8.9 Hz, 2H), 5.55(s, 2H),4.18–4.11 (m, 2H), 3.02 (s, 6H), 3.00–2.94 (m, 2H), 2.05–1.96 (m, 2H). ESI-MS *m/z* calcd $C_{21}H_{22}N_4O$ [M + H]$^+$ 347.2, found 347.2.

(*E*)-3-(Diethylamino)-*N*-(4-((6-(3-(diethylamino)propanamido)-9-oxo-1,2-dihydropyrrolo[2,1-*b*]quinazolin-3(9*H*)-ylidene)methyl)-phenyl)propanamide (7a). A suspension of compound **4a** (0.15 g, 0.50 mmol) in 3-chloropropanoyl chloride (10 mL) was heated under reflux for 4 h, until TLC indicated completion of reaction. After cooling to 0–5 °C, the mixture was filtered, and the crude solid was washed with three 15 mL portions of ether to give an intermediate. To a stirred refluxing suspension of this intermediate and KI (0.05 g) in EtOH (5 mL) was added dropwise pyrrolidine (0.35 mL, 5.0 mmol) in EtOH (5 mL). The mixture was stirred under reflux for 3 h, and 20 mL cool water was added. The solution was filtered, and washed with ether (10 mL). After recrystallization from $CHCl_3$-EtOH (2 : 1 v/v), compound **7a** was obtained as a pale-yellow solid with a yield of 69%. Mp: 179–182 °C.^{1}H NMR (400 MHz, $CDCl_3$) δ 11.74 (s, 1H), 11.57 (s, 1H), 8.22 (d, J = 8.6 Hz, 1H), 7.83–7.78 (m, 2H), 7.73 (dd, J = 8.6, 1.8 Hz, 1H), 7.63 (d, J = 8.6 Hz, 2H), 7.53 (d, J = 8.6 Hz, 2H), 4.28 (d, J = 6.9 Hz, 2H), 3.33–3.23 (m, J = 6.1 Hz, 2H), 2.85–2.77 (m, J = 10.4, 4.8 Hz, 4H), 2.77–2.65 (m, J = 7.2 Hz, 8H), 2.59–2.51 (m, 4H), 1.23–1.12 (m, J = 7.0 Hz, 12H). ^{13}C NMR (101 MHz, $CDCl_3$) δ 171.30, 171.06, 160.85, 156.23, 151.02, 144.26, 139.51, 130.81, 130.39, 129.95, 127.45, 119.48, 118.23, 116.37, 115.41, 48.83, 46.00, 43.96, 33.20, 25.54, 11.47. HRMS *m/z* calcd $C_{32}H_{42}N_6O_3$ [M + Na]$^+$ 581.3216, found 581.3227.

(*E*)-*N*-(4-((11-Oxo-3-(2-(pyrrolidin-1-yl)acetamido)-7,8,9,11-tetrahydro-6*H*-pyrido[2,1-*b*]quinazolin-6-ylidene)methyl)phenyl)-2-(pyrrolidin-1-yl)acetamide (7b). The method for the preparation of compound **7a** was used, replacing **4a** with **4b**, and replacing 3-chloropropanoyl chloride with chloracetyl chloride. Compound **7b** was synthesized as a pale-yellow solid with a yield of 60%. Mp: 96–98 °C. ^{1}H NMR (400 MHz, $CDCl_3$) δ 9.45 (s, 1H), 9.25 (s, 1H), 8.18–8.26 (m, 2H), 7.96 (d, J = 1.8 Hz, 1H), 7.62–7.71 (m, 3H), 7.48 (d, J = 8.5 Hz, 2H), 4.19–4.11 (m, 2H), 3.33 (d, J = 9.2 Hz, 4H), 2.90–3.00 (m, 2H), 2.63–2.80 (m, 8H), 1.98–2.08 (m, 2H), 1.82–1.94 (m, 8H). ^{13}C NMR (101 MHz, $CDCl_3$) δ 169.50, 161.67, 152.36, 148.70, 142.92, 137.73, 135.06, 132.02, 131.03, 128.91, 127.81, 119.21, 118.04, 116.06, 115.49, 59.78, 54.62, 42.02, 25.90, 24.09, 22.00. HRMS *m/z* calcd $C_{31}H_{36}N_6O_3$ [M + Na]$^+$ 563.2747, found 563.2727.

(*E*)-*N*-(4-((11-Oxo-3-(2-(piperidin-1-yl)acetamido)-7,8,9,11-tetrahydro-6*H*-pyrido[2,1-*b*]quinazolin-6-ylidene)methyl)phenyl)-2-(piperidin-1-yl)acetamide (7c). The method for the preparation of compound **7b** was used, replacing pyrrolidine with piperidine. Compound **7c** was synthesized as a pale-yellow solid with a yield of 62%. Mp: 124–125 °C. ^{1}H NMR (400 MHz, $CDCl_3$) δ 9.64 (s, 1H), 9.43 (s, 1H), 8.26–8.18 (m, 2H), 7.93 (d, J = 2.0 Hz, 1H), 7.71–7.62 (m, 3H), 7.48 (d, J = 8.6 Hz, 2H), 4.20–4.11 (m, 2H), 3.12 (d, J = 7.9 Hz, 4H), 2.96 (t, J = 5.5 Hz, 2H), 2.68–2.48 (m, 8H), 2.09–1.99 (m, 2H), 1.71–1.65 (m, 8H), 1.56–1.46 (m, 4H). ^{13}C NMR (101 MHz, $CDCl_3$) δ 169.30, 161.67, 152.45, 148.74, 142.93, 137.74, 135.10, 132.03, 131.08, 128.98, 127.92, 119.11, 117.99, 116.10, 115.38, 62.81, 54.95, 42.03, 26.35, 25.92, 23.61, 22.04. HRMS *m/z* calcd $C_{33}H_{40}N_6O_3$ [M + Na]$^+$ 591.3060, found 591.3053.

(*E*)-2-(Diethylamino)-*N*-(4-((3-(2-(diethylamino)acetamido)-11-oxo-7,8,9,11-tetrahydro-6*H*-pyrido[2,1-*b*]quinazolin-6-ylidene)methyl)phenyl)acetamide (7d). The method for the preparation of compound **7b** was used, replacing pyrrolidine with diethylamine. Compound **7d** was synthesized as a pale-yellow solid with a yield of 58%. Mp: 110–112 °C. ^{1}H NMR (400 MHz, $CDCl_3$) δ 9.74 (s, 1H), 9.54 (s, 1H), 8.26–8.18 (m, 2H), 7.93 (s, 1H), 7.71–7.63 (m, 3H), 7.48 (d, J = 8.2 Hz, 2H), 4.18–4.11 (m, 2H), 3.21 (s, 4H), 2.96 (t, J = 6.1 Hz, 2H), 2.77–2.60 (m, 8H), 2.07–1.99 (m, 2H), 1.12 ppm (t, J = 6.9 Hz, 12H). ^{13}C NMR (101 MHz, $CDCl_3$) δ 170.42, 161.67, 152.40, 148.74, 142.87, 137.69, 135.08, 132.03, 131.07, 128.96, 127.93, 119.03, 117.92, 116.10, 115.32, 58.16, 48.91, 42.02, 25.91, 22.03, 12.46. HRMS *m/z* calcd $C_{31}H_{40}N_6O_3$ [M + Na]$^+$ 567.3060, found 567.3051.

(*E*)-*N*-(4-((11-Oxo-3-(3-(pyrrolidin-1-yl)propanamido)-7,8,9,11-tetrahydro-6*H*-pyrido[2,1-*b*]quinazolin-6-ylidene)methyl)phenyl)-3-(pyrrolidin-1-yl)propanamide (7e). The method for the preparation of compound **7b** was used, replacing chloroacetyl chloride with 3-chloropropionyl chloride. Compound **7e** was synthesized as a pale-yellow solid with a yield of 73%. Mp: 146–148 °C. ^{1}H NMR (400 MHz, $CDCl_3$) δ 11.68 (s, 1H), 11.45 (s, 1H), 8.23–8.13 (m, 2H), 7.83 (d, J = 1.8 Hz, 1H), 7.62–7.51 (m, 3H), 7.45 (d, J = 8.5 Hz, 2H), 4.18–4.10 (m, 2H), 2.95 (t, J = 5.6 Hz, 2H), 2.92–2.84 (m, 4H), 2.78–2.65 (m, 8H), 2.61–2.53 (m, 4H), 2.06–2.00 (m, 2H), 1.98–1.88 (m, 8H). ^{13}C NMR (101 MHz, $CDCl_3$) δ 171.31, 171.02, 161.69, 152.50, 148.76, 144.24, 138.98, 135.24, 131.54, 131.07, 128.80, 127.73, 119.33, 118.52, 115.70,

115.57, 53.16, 51.33, 41.94, 34.73, 25.95, 23.76, 22.11. HRMS *m/z* calcd $C_{33}H_{40}N_6O_3$ $[M + Na]^+$ 591.3060, found 591.3065.

(*E*)-*N*-(4-((11-Oxo-3-(3-(piperidin-1-yl)propanamido)-7,8,9,11-tetrahydro-6*H*-pyrido[2,1-*b*]quinazolin-6-ylidene)methyl)phenyl)-3-(piperidin-1-yl)propanamide (7f). The method for the preparation of compound **7e** was used, replacing pyrrolidine with piperidine. Compound **7f** was synthesized as a pale-yellow solid with a yield of 76%. Mp: 142–143 °C. ^{1}H NMR (400 MHz, $CDCl_3$) δ 11.77 (s, 1H), 11.60 (s, 1H), 8.23–8.14 (m, 2H), 7.97–7.90 (m, 1H), 7.66–7.55 (m, *J* = 8.5 Hz, 3H), 7.47 (d, *J* = 8.5 Hz, 2H), 4.18–4.11 (m, 2H), 2.96 (t, *J* = 5.7 Hz, 2H), 2.80–2.46 (m, 16H), 2.07–2.01 (m, 2H), 1.81–1.70 (m, 8H), 1.67–1.50 (m, 4H). ^{13}C NMR (101 MHz, $CDCl_3$) δ 171.25, 170.96, 161.68, 152.45, 148.81, 144.20, 139.01, 135.25, 131.50, 131.10, 128.77, 127.71, 119.15, 118.36, 115.60, 54.24, 53.64, 41.93, 32.61, 26.24, 25.94, 24.17, 22.09. HRMS *m/z* calcd $C_{35}H_{44}N_6O_3$ $[M + H]^+$ 597.3567, found 597.3553.

(*E*)-3-(Diethylamino)-*N*-(4-((3-(3-(diethylamino)propanamido)-11-oxo-7,8,9,11-tetrahydro-6*H*-pyrido[2,1-*b*]quinazolin-6-ylidene)-methyl)phenyl)propanamide (7g). The method for the preparation of compound **7e** was used, replacing pyrrolidine with diethylamine. Compound **7g** was synthesized as a pale-yellow solid with a yield of 70%. Mp: 101–104 °C. ^{1}H NMR (400 MHz, $CDCl_3$) δ 11.69 (s, 1H), 11.45 (s, 1H), 8.19 (d, *J* = 8.7 Hz, 1H), 8.16 (s, 1H), 7.85 (d, *J* = 1.8 Hz, 1H), 7.63 (dd, *J* = 8.7, 1.8 Hz, 1H), 7.60 (d, *J* = 8.6 Hz, 2H), 7.45 (d, *J* = 8.6 Hz, 2H), 4.18–4.10 (m, 2H), 2.95 (t, *J* = 5.5 Hz, 2H), 2.86–2.78 (m, 4H), 2.78–2.66 (m, 8H), 2.61–2.51 (m, 4H), 2.05–1.98 (m, 2H), 1.24–1.10 (m, 12H). ^{13}C NMR (101 MHz, $CDCl_3$) δ 171.20, 170.87, 161.65, 152.44, 148.78, 144.08, 138.85, 135.20, 131.54, 131.06, 128.79, 127.74, 119.15, 118.35, 115.71, 115.41, 48.86, 46.00, 41.90, 33.20, 25.92, 22.10, 11.34. HRMS *m/z* calcd $C_{33}H_{44}N_6O_3$ $[M + Na]^+$ 595.3373, found 595.3386.

(*E*)-*N*-(4-((12-Oxo-3-(3-(pyrrolidin-1-yl)propanamido)-7,8,9,10-tetrahydroazepino[2,1-*b*]quinazolin-6(12*H*)-ylidene)methyl)phenyl)-3-(pyrrolidin-1-yl)propanamide (7h). The method for the preparation of compound **7e** was used, replacing compound **4b** with compound **4c**. Compound **7h** was synthesized as a pale-yellow solid with a yield of 57%. Mp: 138–140 °C. ^{1}H NMR (400 MHz, $CDCl_3$) δ 11.61 (s, 1H), 11.32 (s, 1H), 8.14 (d, *J* = 8.7 Hz, 1H), 7.70 (d, *J* = 8.7 Hz, 1H), 7.66 (s, 1H), 7.47 (d, *J* = 8.4 Hz, 2H), 7.38 (d, *J* = 8.4 Hz, 2H), 6.98 (s, 1H), 4.27–4.16 (m, 2H), 2.85–2.77 (m, 4H), 2.76–2.70 (m, 2H), 2.68–2.59 (m, 8H), 2.53–2.47 (m, 4H), 1.89–1.77 (m, 12H). ^{13}C NMR (101 MHz, $CDCl_3$) δ 170.30, 169.94, 160.14, 158.38, 147.98, 143.34, 137.69, 134.82, 132.55, 130.20, 129.44, 127.00, 118.36, 117.91, 115.25, 114.73, 52.14, 50.31, 41.39, 33.69, 27.94, 25.08, 23.21, 22.72. HRMS *m/z* calcd $C_{32}H_{42}N_6O_3$ $[M + Na]^+$ 605.3216, found 605.3242.

(*E*)-*N*-(4-((12-Oxo-3-(3-(piperidin-1-yl)propanamido)-7,8,9,10-tetrahydroazepino[2,1-*b*]quinazolin-6(12*H*)-ylidene)methyl)phenyl)-3-(piperidin-1-yl)propanamide (7i). The method for the preparation of compound **7h** was used, replacing pyrrolidine with piperidine. Compound **7i** was synthesized as a pale-yellow solid with a yield of 55%. Mp: 145–147 °C. ^{1}H NMR (400 MHz, $CDCl_3$) δ 11.72 (s, 1H), 11.53 (s, 1H), 8.23 (d, *J* = 8.7 Hz, 1H), 7.84 (s, 1H), 7.77 (s, *J* = 8.7 Hz, 1H), 7.60 (d, *J* = 8.3 Hz, 2H), 7.47 (d, *J* = 8.3 Hz, 2H), 7.07 (s, 1H), 4.33–4.24 (m, 2H), 2.86–2.79 (m, 2H), 2.72–2.66 (m, 4H), 2.65–2.48 (m, 12H), 1.95–1.85 (m, 4H), 1.77–1.70 (m, 8H), 1.62–1.53 (m, 4H). ^{13}C NMR (101 MHz, $CDCl_3$) δ 171.23, 170.88, 161.17, 159.35, 149.10, 144.3, 138.76, 135.81, 133.63, 131.21, 130.50, 127.99, 119.20, 118.82, 116.30, 115.73, 54.24, 53.65, 42.39, 32.61, 28.98, 26.19, 26.10,24.21, 24.12. HRMS *m/z* calcd $C_{36}H_{46}N_6O_3$ $[M + Na]^+$ 633.3529, found 633.3544.

(*E*)-3-(Diethylamino)-*N*-(4-((7-(3-(diethylamino)propanamido)-9-oxo-1,2-dihydropyrrolo[2,1-*b*]quinazolin-3(9*H*)-ylidene)methyl)-phenyl)propanamide (7j). The method for the preparation of compound **7a** was used, replacing compound **4a** with compound **4d**. Compound **7j** was synthesized as a pale-yellow solid with a yield of 67%. Mp: 220–222 °C. ^{1}H NMR (400 MHz, $CDCl_3$) δ 11.63 (s, 1H), 11.57 (s, 1H), 8.29 (dd, *J* = 8.9, 2.1 Hz, 1H), 8.09 (s, *J* = 2.1 Hz, 1H), 7.77 (s, 1H), 7.72 (d, *J* = 8.9 Hz, 1H), 7.63 (d, *J* = 8.4 Hz, 2H), 7.52 (d, *J* = 8.4 Hz, 2H), 4.29 (t, *J* = 7.1 Hz, 2H), 3.29 (d, *J* = 7.1 Hz, 2H), 2.85–2.77 (m, 4H), 2.77–2.66 (m, 8H), 2.58–2.51 (m, 4H), 1.21–1.13 (m, 12H). ^{13}C NMR (101 MHz, $CDCl_3$) δ 171.12, 160.99, 154.63, 145.92, 139.47, 137.21, 130.86, 130.75, 129.86, 129.81, 128.11, 126.91, 121.17, 119.50, 114.98, 48.86, 46.00, 44.02, 33.13, 25.58, 11.52. HRMS *m/z* calcd $C_{32}H_{42}N_6O_3$ $[M + H]^+$ 559.3397, found 559.3390.

(*E*)-*N*-(4-((11-Oxo-2-(2-(pyrrolidin-1-yl)acetamido)-7,8,9,11-tetrahydro-6*H*-pyrido[2,1-*b*]quinazolin-6-ylidene)methyl)phenyl)-2-(pyrrolidin-1-yl)acetamide (7k). The method for the preparation of compound **7b** was used, replacing **4b** with **4e**. Compound **7k** was synthesized as a pale-yellow solid with a yield of 52%. Mp: 113–115 °C. ^{1}H NMR (400 MHz, $CDCl_3$) δ 9.46 (s, 1H), 9.26 (s, 1H), 8.41 (dd, *J* = 8.9, 2.3 Hz, 1H), 8.15 (s, 1H), 8.07 (d, *J* = 2.3 Hz, 1H), 7.72 (d, *J* = 8.9 Hz, 1H), 7.66 (d, *J* = 8.5 Hz, 2H), 7.47 (d, *J* = 8.5 Hz, 2H), 4.23–4.12 (m, 2H), 3.38–3.27 (m, 4H), 2.97 (t, *J* = 5.6 Hz, 2H), 2.81–2.67 (m, 8H), 2.11–1.98 (m, 2H), 1.94–1.86 (m, 8H). ^{13}C NMR (101 MHz, $CDCl_3$) δ 168.32, 160.88, 149.88, 143.14, 136.70, 135.19, 133.57, 131.07, 129.98, 128.04, 127.38, 125.60, 119.32, 118.19, 114.21, 58.73, 53.65, 41.24, 24.90, 23.11, 21.06. HRMS *m/z* calcd $C_{31}H_{36}N_6O_3$ $[M + Na]^+$ 563.2750, found 563.2750.

(*E*)-*N*-(4-((11-Oxo-2-(2-(piperidin-1-yl)acetamido)-7,8,9,11-tetrahydro-6*H*-pyrido[2,1-*b*]quinazolin-6-ylidene)methyl)phenyl)-2-(piperidin-1-yl)acetamide (7l). The method for the preparation of compound **7c** was used, replacing compound **4b** with compound **4e**. Compound **7l** was synthesized as a pale-yellow solid with a yield of 53%. Mp: 169–173 °C. ^{1}H NMR (400 MHz, $CDCl_3$) δ 9.61 (s, 1H), 9.46 (s, 1H), 8.39 (dd, *J* = 8.9, 2.3 Hz, 1H), 8.16 (s, 1H), 8.09 (s, *J* = 2.3 Hz, 1H), 7.72 (d, *J* = 8.9 Hz, 1H), 7.66 (d, *J* = 8.5 Hz, 2H), 7.48 (d, *J* = 8.5 Hz, 2H), 4.21–4.14 (m, 2H), 3.23–3.07 (m, 4H), 2.97 (t, *J* = 5.6 Hz, 2H), 2.69–2.52 (m, 8H), 2.08–2.00 (m, 2H), 1.77–1.64 (m, 8H), 1.57–1.48 (m, 4H). ^{13}C NMR (101 MHz, $CDCl_3$) δ 168.87, 161.86, 150.98, 144.17, 137.68, 136.15, 134.57, 132.17, 130.98, 129.07, 128.38, 126.58, 120.36, 119.12, 115.19, 62.71, 54.94, 42.25, 26.19, 25.89, 23.54, 22.06. HRMS *m/z* calcd $C_{33}H_{40}N_6O_3$ $[M + Na]^+$ 591.3060, found 591.3060.

(*E*)-2-(Diethylamino)-*N*-(4-((2-(2-(diethylamino)acetamido)-11-oxo-7,8,9,11-tetrahydro-6*H*-pyrido[2,1-*b*]quinazolin-6-ylidene)methyl)phenyl)acetamide (7m). The method for the preparation of compound **7d** was used, replacing **4b** with **4e**. Compound **7m** was synthesized as a pale-yellow solid with a yield of 53%. Mp: 107–108 °C. ^{1}H NMR (400 MHz, $CDCl_3$) δ 9.72 (s, 1H), 9.54 (s, 1H),

 This journal is © The Royal Society of Chemistry 2011

8.41 (dd, J = 8.9, 2.3 Hz, 1H), 8.16 (s, 1H), 8.06 (s, J = 2.3 Hz, 1H), 7.73 (d, J = 8.9 Hz, 1H), 7.66 (d, J = 8.6 Hz, 2H), 7.48 (d, J = 8.6 Hz, 2H), 4.20–4.13 (m, 2H), 3.25–3.12 (m, J = 4.5 Hz, 4H), 3.00–2.93 (m, 2H), 2.74–2.61 (m, 8H), 2.08–1.99 (m, 2H), 1.15–1.08 (m, 12H). ^{13}C NMR (101 MHz, $CDCl_3$) δ 170.31, 161.90, 150.87, 144.16, 137.67, 136.16, 134.59, 132.08, 131.03, 129.07, 128.44, 126.48, 120.38, 119.04, 115.06, 58.11, 48.96, 42.28, 25.92, 22.09, 12.45. HRMS m/z calcd $C_{31}H_{40}N_6O_3$ [M + Na]$^+$ 567.3060, found 567.3060.

(*E*)-*N*-(4-((11-Oxo-2-(3-(pyrrolidin-1-yl)propanamido)-7,8,9,11-tetrahydro-6*H*-pyrido[2,1-*b*]quinazolin-6-ylidene)methyl)phenyl)-3-(pyrrolidin-1-yl)propanamide (7n). The method for the preparation of compound **7e** was used, replacing compound **4b** with compound **4e**. Compound **7n** was synthesized as a pale-yellow solid with a yield of 65%. Mp: 192–194 °C. ^{1}H NMR (400 MHz, $CDCl_3$) δ 11.56 (s, 1 H), 11.45 (s, 1H), 8.24 (dd, J = 8.8, 1.9 Hz, 1H), 8.13 (s, 1H), 8.01 (d, J = 1.9 Hz, 1H), 7.69 (d, J = 8.8 Hz, 1H), 7.55 (d, J = 8.4 Hz, 2H), 7.44 (d, J = 8.4 Hz, 2H), 4.22–4.09 (m, 2H), 3.01–2.93 (m, 2H), 2.93–2.83 (m, 4H), 2.78–2.65 (m, 8H), 2.63–2.52 (m, 4H), 2.06–1.99 (m, 2H), 1.96–1.89 (m, 8H). ^{13}C NMR (101 MHz, $CDCl_3$) δ 170.89, 161.86, 150.72, 143.86, 138.88, 137.24, 134.57, 131.57, 130.97, 128.83, 128.18, 127.10, 120.33, 119.31, 115.35, 53.18, 51.36, 42.17, 34.61, 25.92, 23.75, 22.10. HRMS m/z calcd $C_{33}H_{40}N_6O_3$ [M + Na]$^+$ 591.3060, found 591.3057.

(*E*)-*N*-(4-((11-Oxo-2-(3-(piperidin-1-yl)propanamido)-7,8,9,11-tetrahydro-6*H*-pyrido[2,1-*b*]quinazolin-6-ylidene)methyl)phenyl)-3-(piperidin-1-yl)propanamide (7o). The method for the preparation of compound **7f** was used, replacing compound **4b** with compound **4e**. Compound **7o** was synthesized as a pale-yellow solid with a yield of 67%. Mp: 198–199 °C. ^{1}H NMR (400 MHz, $CDCl_3$) δ 11.71 (s, 1H), 11.55 (s, 1H), 8.28 (dd, J = 8.9, 2.1 Hz, 1H), 8.13 (s, 1H), 8.09 (s, J = 2.1 Hz, 1H), 7.70 (d, J = 8.9 Hz, 1H), 7.61 (d, J = 8.4 Hz, 2H), 7.45 (d, J = 8.4 Hz, 2H), 4.22–4.10 (m, 2H), 2.96 (t, J = 6.0 Hz, 2H), 2.78–2.43 (m, 16H), 2.07–1.99 (m, 2H), 1.80–1.70 (m, 8H), 1.64–1.53 (m, 4H). ^{13}C NMR (101 MHz, $CDCl_3$) δ 170.89, 161.88, 150.75, 143.85, 138.96, 137.34, 134.60, 131.57, 131.04, 128.85, 128.26, 126.92, 120.40, 119.18, 115.15, 54.30, 53.68, 42.18, 32.56, 26.22, 25.96, 24.17, 22.14. HRMS m/z calcd $C_{35}H_{44}N_6O_3$ [M + Na]$^+$ 619.3373, found 619.3391.

(*E*)-3-(Diethylamino)-*N*-(4-((2-(3-(diethylamino)propanamido)-11-oxo-7,8,9,11-tetrahydro-6*H*-pyrido[2,1-*b*]quinazolin-6-ylidene)-methyl)phenyl)propanamide (7p). The method for the preparation of compound **7g** was used, replacing compound **4b** with compound **4e**. Compound **7p** was synthesized as a pale-yellow solid with a yield of 64%. Mp: 173–174 °C. ^{1}H NMR (400 MHz, $CDCl_3$) δ 11.61 (s, 1H), 11.47 (s, 1H), 8.29 (dd, J = 8.9, 2.3 Hz, 1H), 8.13 (s, 1H), 8.04 (d, J = 2.3 Hz, 1H), 7.69 (d, J = 8.9 Hz, 1H), 7.59 (d, J = 8.5 Hz, 2H), 7.44 (d, J = 8.5 Hz, 2H), 4.19–4.11 (m, 2H), 2.95 (t, J = 5.8 Hz, 2H), 2.84–2.76 (m, 4H), 2.76–2.65 (m, 8H), 2.59–2.49 (m, 4H), 2.07–1.98 (m, 2H), 1.22–1.11 (m, 12H).^{13}C NMR (101 MHz, $CDCl_3$) δ 171.02, 161.87, 150.71, 143.85, 138.80, 137.18, 134.57, 131.55, 130.99, 128.80, 128.23, 126.95, 120.37, 119.14, 115.05, 48.87, 46.01, 42.16, 33.12, 25.92, 22.11, 11.44. HRMS m/z calcd $C_{33}H_{44}N_6O_3$ [M + H]$^+$ 573.3508, found 573.3571.

(*E*)-*N*-(3-(4-(Dimethylamino)benzylidene)-9-oxo-1,2,3,9-tetrahydropyrrolo[2,1-*b*]quinazolin-6-yl)-3-(pyrrolidin-1-yl)propanamide (7q). The method for the preparation of compound **7a** was used, replacing diethylamide with pyrrolidine, and replacing compound **4a** with compound **6a**. Compound **7q** was synthesized as a yellow solid with a yield of 65%. Mp: 194–196 °C. ^{1}H NMR (400 MHz, $CDCl_3$) δ 11.49 (s, 1H), 8.20 (d, J = 8.7 Hz, 1H), 7.76 (s, 1H), 7.73 (d, J = 1.9 Hz, 1H), 7.68 (dd, J = 8.7, 1.9 Hz, 1H), 7.49 (d, J = 8.9 Hz, 2H), 6.75 (d, J = 8.9 Hz, 2H), 4.26 (t, J = 6.9 Hz, 2H), 3.29–3.23 (m, 2H), 3.04 (s, 6H), 2.96–2.91 (m, 2H), 2.82–2.73 (m, 4H), 2.67–2.59 (m, 2H), 2.00–1.94 (m, 4H). ^{13}C NMR (101 MHz, $CDCl_3$) δ 171.34, 161.02, 156.94, 151.21, 150.59, 144.30, 131.62, 131.33, 127.39, 125.81, 123.64, 117.94, 116.21, 115.36, 111.94, 53.18, 51.34, 44.00, 40.12, 34.80, 25.54, 23.78. HRMS m/z calcd $C_{27}H_{31}N_5O_2$ [M + H]$^+$ 458.2556, found 458.2552.

(*E*)-*N*-(3-(4-(Dimethylamino)benzylidene)-9-oxo-1,2,3,9-tetrahydropyrrolo[2,1-*b*]quinazolin-6-yl)-3-(piperidin-1-yl)propanamide (7r). The method for the preparation of compound **7q** was used, replacing pyrrolidine with piperidine. Compound **7r** was synthesized as a yellow solid with a yield of 61%. Mp: 202–204 °C. ^{1}H NMR (400 MHz, $CDCl_3$) δ 11.58 (s, 1H), 8.13 (d, J = 8.7 Hz, 1H), 7.77 (d, J = 1.9 Hz, 1H), 7.70 (s, 1H), 7.59 (dd, J = 8.7, 1.9 Hz, 1H), 7.41 (d, J = 8.9 Hz, 2H), 6.67 (d, J = 8.9 Hz, 2H), 4.22–4.14 (m, 2H), 3.22–3.14 (m, 2H), 2.96 (s, 6H), 2.67–2.45 (m, 8H), 1.74–1.64 (m, 4H), 1.57–1.47 (m, 2H). ^{13}C NMR (101 MHz, $CDCl_3$) δ 170.14, 159.99, 155.88, 150.30, 149.56, 143.22, 130.60, 130.31, 126.35, 124.82, 122.65, 116.77, 115.23, 114.36, 110.91, 53.22, 52.69, 42.96, 39.10, 31.68, 25.18, 24.53, 23.14. HRMS m/z calcd $C_{28}H_{33}N_5O_2$ [M + H]$^+$ 472.2713, found 472.2711.

(*E*)-*N*-(6-(4-(Dimethylamino)benzylidene)-11-oxo-7,8,9,11-tetrahydro-6*H*-pyrido[2,1-*b*]quinazolin-3-yl)-3-(pyrrolidin-1-yl)propanamide (7s). The method for the preparation of compound **7q** was used, replacing compound **6a** with compound **6b**. Compound **7s** was synthesized as a yellow solid with a yield of 73%. Mp: 181–183 °C. ^{1}H NMR (400 MHz, $CDCl_3$) δ 11.53 (s, 1H), 8.17 (d, J = 8.7 Hz, 1H), 8.13 (s, 1H), 7.82 (d, J = 1.4 Hz, 1H), 7.56 (dd, J = 8.7, 1.4 Hz, 1H), 7.45 (d, J = 8.7 Hz, 2H), 6.73 (d, J = 8.7 Hz, 2H), 4.18–4.08 (m, 2H), 3.02 (s, 6H), 3.00–2.91 (m, 4H), 2.80–2.72 (m, 4H), 2.68–2.60 (m, 2H), 2.08–1.99 (m, 2H), 1.98–1.91 (m, 4H). ^{13}C NMR (101 MHz, $CDCl_3$) δ 171.07, 161.76, 153.22, 150.21, 148.99, 144.06, 136.28, 132.00, 127.70, 125.19, 124.37, 118.10, 115.49, 111.68, 53.24, 51.34, 41.72, 40.18, 34.72, 26.25, 23.73, 22.19. HRMS m/z calcd $C_{28}H_{33}N_5O_2$ [M + H]$^+$ 472.2713, found 472.2714.

(*E*)-*N*-(6-(4-(Dimethylamino)benzylidene)-11-oxo-7,8,9,11-tetrahydro-6*H*-pyrido[2,1-*b*]quinazolin-3-yl)-3-(piperidin-1-yl)propanamide (7t). The method for the preparation of compound **7s** was used, replacing pyrrolidine with piperidine. Compound **7t** was synthesized as a yellow solid with a yield of 74%. Mp: 196–197 °C. ^{1}H NMR (400 MHz, $CDCl_3$) δ 11.66 (s, 1H), 8.18 (d, J = 8.7 Hz, 1H), 8.15 (s, 1H), 7.91 (d, J = 1.8 Hz, 1H), 7.56 (dd, J = 8.7, 1.8 Hz, 1H), 7.46 (d, J = 8.8 Hz, 2H), 6.74 (d, J = 8.8 Hz, 2H), 4.17–4.10 (m, 2H), 3.03 (s, 6H), 2.97 (t, J = 5.8 Hz, 2H), 2.74–2.69 (m, 2H), 2.67–2.51 (m, 6H), 2.04–1.98 (m, 2H), 1.80–1.73 (m, 4H), 1.64–1.52 (m, 2H). ^{13}C NMR (101 MHz, $CDCl_3$) δ 171.20, 161.77, 153.19, 150.21, 149.07, 144.09, 136.30, 132.00,

127.71, 125.24, 124.39, 117.97, 115.46, 111.68, 54.25, 53.69, 41.71, 40.18, 32.69, 26.24, 24.16, 22.20. HRMS *m/z* calcd $C_{29}H_{35}N_5O_2$ $[M + H]^+$ 486.2869, found 486.2864.

(*E*)-*N*-(3-(4-(Dimethylamino)benzylidene)-9-oxo-1,2,3,9-tetrahydropyrrolo[2,1-*b*]quinazolin-7-yl)-3-(pyrrolidin-1-yl)propanamide (7u). The method for the preparation of compound **7q** was used, replacing compound **6a** with compound **6c**. Compound **7u** was synthesized as a yellow solid with a yield of 58%. Mp: 240–242 °C. ^{1}H NMR (400 MHz, $CDCl_3$) δ 11.39 (s, 1H), 8.21 (dd, J = 8.9, 2.1 Hz, 1H), 8.05 (d, J = 2.1 Hz, 1H), 7.74 (s, 1H), 7.69 (d, J = 8.9 Hz, 1H), 7.48 (d, J = 8.9 Hz, 2H), 6.75 (d, J = 8.9 Hz, 2H), 4.30–4.24 (m, 2H), 3.31–3.24 (m, 2H), 3.04 (s, 6H), 2.95–2.89 (m, 2H), 2.81–2.70 (m, 4H), 2.65–2.58 (m, 2H), 1.98–1.92 (m, 4H). ^{13}C NMR (101 MHz, $CDCl_3$) δ 171.02, 161.12, 155.36, 150.54, 146.27, 136.77, 131.52, 130.74, 127.81, 127.01, 125.79, 123.73, 120.87, 115.32, 111.97, 53.24, 51.42, 44.04, 40.14, 34.60, 25.57, 23.75. HRMS *m/z* calcd $C_{27}H_{31}N_5O_2$ $[M + H]^+$ 458.2556, found 458.2543.

(*E*)-*N*-(3-(4-(Dimethylamino)benzylidene)-9-oxo-1,2,3,9-tetrahydropyrrolo[2,1-*b*]quinazolin-7-yl)-3-(piperidin-1-yl)propanamide (7v). The method for the preparation of compound **7u** was used, replacing pyrrolidine with piperidine. Compound **7v** was synthesized as a yellow solid with a yield of 56%. Mp: 243–245 °C. ^{1}H NMR (400 MHz, $CDCl_3$) δ 11.60 (s, 1H), 8.18 (dd, J = 8.9, 2.4 Hz, 1H), 8.03 (d, J = 2.4 Hz, 1H), 7.66 (s, 1H), 7.62 (d, J = 8.9 Hz, 1H), 7.41 (d, J = 8.8 Hz, 2H), 6.67 (d, J = 8.8 Hz, 2H), 4.24–4.14 (m, 2H), 3.24–3.15 (m, 2H), 2.96 (s, 6H), 2.69–2.39 (m, 8H), 1.74–1.62 (m, 4H), 1.55–1.45 (m, 2H). ^{13}C NMR (101 MHz, $CDCl_3$) δ 169.88, 160.07, 154.29, 149.50, 145.18, 135.84, 130.48, 129.67, 126.83, 125.73, 124.78, 122.71, 119.88, 114.04, 110.94, 53.28, 52.6, 42.98, 39.10, 31.48, 25.22, 24.55, 23.19. HRMS *m/z* calcd $C_{28}H_{33}N_5O_2$ $[M + H]^+$ 472.2713, found 472.2705.

(*E*)-*N*-(6-(4-(Dimethylamino)benzylidene)-11-oxo-7,8,9,11-tetrahydro-6*H*-pyrido[2,1-*b*]quinazolin-2-yl)-3-(pyrrolidin-1-yl)propanamide (7w). The method for the preparation of compound **7u** was used, replacing compound **6c** with compound **6d**. Compound **7w** was synthesized as a yellow solid with a yield of 60%. Mp: 218–220 °C. ^{1}H NMR (400 MHz, $CDCl_3$) δ 11.26 (s, 1H), 8.20 (dd, J = 8.9, 2.3 Hz, 1H), 8.10 (s, 1H), 8.04 (d, J = 2.3 Hz, 1H), 7.67 (d, J = 8.9 Hz, 1H), 7.45 (d, J = 8.8 Hz, 2H), 6.74 (d, J = 8.8 Hz, 2H), 4.21–4.11 (m, 2H), 3.03 (s, 6H), 3.01–2.92 (m, 4H), 2.85–2.73 (m, 4H), 2.70–2.60 (m, 2H), 2.07–1.99 (m, 2H), 1.99–1.91 (m, 4H). ^{13}C NMR (101 MHz, $CDCl_3$) δ 168.99, 161.92, 151.60, 150.15, 144.43, 136.27, 135.63, 131.92, 127.93, 126.99, 125.23, 124.41, 119.90, 115.77, 111.68, 53.83, 51.37, 41.98, 40.16, 33.89, 26.21, 23.52, 22.13. HRMS *m/z* calcd $C_{28}H_{33}N_5O_2$ $[M + H]^+$ 472.2713, found 472.2718.

(*E*)-*N*-(6-(4-(Dimethylamino)benzylidene)-11-oxo-7,8,9,11-tetrahydro-6*H*-pyrido[2,1-*b*]quinazolin-2-yl)-3-(piperidin-1-yl)propanamide (7x). The method for the preparation of compound **7w** was used, replacing pyrrolidine with piperidine. Compound **7x** was synthesized as a yellow solid with a yield of 62%. Mp: 215–217 °C. ^{1}H NMR (400 MHz, $CDCl_3$) δ 11.48 (s, 1H), 8.27–8.08 (m, 3H), 7.70–7.64 (m, 1H), 7.45 (d, J = 8.9 Hz, 2H), 6.74 (d, J = 8.9 Hz, 2H), 4.19–4.12 (m, 2H), 3.03 (s, 6H), 3.01–2.95 (m, 2H), 2.87–2.76 (m, 2H), 2.73–2.58 (m, 4H), 2.06–1.98 (m, 2H), 1.86–1.72 (m, 4H), 1.65–1.51 (m, 4H). ^{13}C NMR (101 MHz, $CDCl_3$) δ 170.34, 161.89, 151.53, 150.16, 144.22, 136.72, 135.62, 131.89, 128.03, 126.86, 125.27, 124.41, 120.04, 115.30, 111.68, 54.15, 53.72, 41.94, 40.16, 32.44, 26.22, 25.67, 23.83, 22.19. HRMS *m/z* calcd $C_{29}H_{35}N_5O_2$ $[M + H]^+$ 486.2869, found 486.2874.

Biological activity and molecular modeling

FRET-melting assay. FRET assay was carried out on a real-time PCR apparatus following previously published procedures. The fluorescently labeled oligonucleotide F21T [5′-FAM-d(GGG[TTAGGG]$_3$)-TAMRA-3′] and F10T [5′-FAM-dTATAGCTATA-HEG-TATA-GCTATA-TAMRA-3′] (HEG linker: [(-CH_2-CH_2-*O*-)$_6$]) were used as G-quadruplex and duplex model respectively. Fluorescence melting curves were determined with a Roche LightCycler 2 real-time PCR machine, using a total reaction volume of 20 μL, with 0.2 μM of labeled oligonucleotide in Tris-HCl buffer (10 mM, pH 7.2) containing 60 mM KCl. Fluorescence readings with excitation at 470 nm and detection at 530 nm were taken at intervals of 1 °C over the range 37–99 °C, with a constant temperature being maintained for 30 s prior to each reading to ensure a stable value. The melting of the G-quadruplex was monitored alone or in the presence of various concentrations of compounds and/or of double-stranded competitor ds26 [5′-GTTAGCCTAGCTTAAGCTAGGCTAAC-3′]. Final analysis of the data was carried out using Origin 7.5 (OriginLab Corp.).

CD measurements

The oligomer HTG21 [5′-d(GGG[TTAGGG]$_3$)-3′] was diluted from stock to the required concentration (5 μM) in Tris-HCl buffer (10 mM, pH 7.2) with or without 150 mM KCl, and then annealed by heating to 90 °C for 5 min, gradually cooled to room temperature, and incubated at 4 °C overnight. CD experiments were performed on a Chirascan circular dichroism spectrophotometer (Applied Photophysics). A quartz cuvette with 4 mm path length was used for the spectra recorded over a wavelength range of 230–450 nm at 1 nm bandwidth, 1 nm step size, and 0.5 s time per point. A buffer baseline was collected in the same cuvette, and subtracted from the sample spectra. Final analysis of the data was carried out using Origin 7.5 (OriginLab Corp.).

Surface plasmon resonance

SPR measurements were performed on a ProteOn XPR36 Protein Interaction Array system (Bio-Rad Laboratories, Hercules, CA) using a Neutravidin-coated GLH sensor chip. Oligonucleotides used were Biotin-Htelo (Quadruplex): 5-biotin-[(GTTAGG)$_5$]-3, Biotin-Atelo (single-stranded control): 5-biotin-[(AGTTAG)$_5$]-3, and Biotin-duplex: 5-biotin-T_9CGAATTCGT$_5$CGAATTCG-3. In a typical experiment, biotinylated DNA was folded in filtered and degassed running buffer (50 mM Tris-HCl, pH 7.2, 100 mM KCl). The DNA samples were then captured (~1000 RU) in flow cell 1, leaving the fourth flow cell as a blank. Ligand solutions were prepared with running buffer through serial dilutions of stock solution. Five concentrations were injected simultaneously at a flow rate of 100 μL min^{-1} for 300 s (or 400 s) of association phase, followed with 300 s (or 400 s) of dissociation phase at 25 °C. The GLH sensor chip was regenerated with short

 This journal is © The Royal Society of Chemistry 2011

injection of 50 mM NaOH between consecutive measurements. The final graphs were obtained by subtracting black and single-stranded control sensorgrams from quadruplex sensorgrams. Data were analyzed with ProteOn manager software, using the kinetic method for kinetic data fitting.

NMR spectroscopy

NMR experiments were performed on a Bruker 600 MHz spectrometer. All of the titration experiments were carried out at 25 °C in a 90% H_2O/10% D_2O solution containing 150 mM KCl and 25 mM potassium phosphate buffer (pH 7.2). The oligonucleotide $d(T_2AG_3)$ was purified by HPLC, and the concentration was 0.5 mM for the NMR measurements.

Molecular modeling

The NMR structure of the mixed hybrid-type 26-mer telomeric G-quadruplex (PDB 2HY9))[45] was used as the initial template to study the interactions between isaindigotone derivatives and telomeric DNA. For comparison with the $d(GGG[TTAGGG]_3)$ DNA used in the FRET and CD experiments, we removed five adenines from 5′ end of the hybrid-type quadruplex to generate the 21-mer structure. Ligand structures were constructed with SYBYL7.3 (Tripos Inc., St Louis, MO, USA) and optimized with GAUSSIAN 03 using the HF/6-31G* basis set.[48] Docking studies were performed using the AUTODOCK 4.0 program.[49] The dimensions of the active site box were chosen to be large enough to encompass the entire DNA molecule. Docking calculations were carried out using the Lamarckian genetic algorithm (LGA). A maximum number of 2,500,000 energy evaluation was used. Each docking experiment was consisted of 100 independent runs. All the MD simulations were performed using the AMBER 10.0 program suite.[50] Based on the electrostatic potential (ESP) calculations at the *ab initio* HF/6-31G* level,[48] the partial atomic charges for ligands were refined by using RESP calculation in antechamber module.[51] Other parameters for ligands were taken from the Generalized Amber Force field (GAFF).[52] Two K^+ ions were placed manually in the central core of the complexes. Every ligand-receptor system was then solvated in a truncated octahedron box of TIP3P water molecules with a 10.0 Å buffer along each dimension. Additional positively-charged counter ions were added in the system to neutralize the negative charge on the DNA backbone. The AMBER ff99 force field[53] was applied for G-quadruplexes, ions, and water molecules. Periodic boundary conditions were applied to avoid the edge effect. The Particle Mesh Ewald (PME) method was used to calculate long-range electrostatic interactions with a 10 Å residue-based cutoff.[54] The hydrogen bonds were constrained using SHAKE algorithm.[55] The final systems were subjected to initial minimization to equilibrate the solvent and counter cations, and were then heated from 0 to 300 K in a 100 ps simulation, and followed with a 100 ps simulation to equilibrate the density. Afterwards, 10 ns constant pressure MD simulation was performed in an NPT ensemble at 1 atm and 300 K. All calculations were carried out with the SANDER module. The MM/PBSA method and NMODE module were used to calculate the binding free energy and the entropic contribution.[56] All the waters and counter-ions were stripped off, but the K^+ ions present within the central channel were included. K^+ radius was set to 2.025 Å.[57] A total of 100 snapshots were taken from the last 2 ns trajectory with an interval of 20 ps. Each snapshot was minimized using the conjugate gradient method for 10,000 steps with a distance-dependent dielectric constant of 4 inter-atomic distances. The terminating criterion for minimization was set to 0.01 kJ mol^{-1} Å gradient RMS. To investigate the heat stability of the ligand-quadruplex complex, we elongated the simulation time for another 2 ns at 350 K.

Acknowledgements

We thank the Natural Science Foundation of China (Grants U0832005, 90813011, 81001400), the International S&T Co-operation Program of China (2010DFA34630), the Specialized Research Fund for the Doctoral Program of Higher Education (20090171110050), and the Science Foundation of Guangzhou (2009A1-E011-6) for financial support of this study.

References

1 J. T. Davis, *Angew. Chem., Int. Ed.*, 2004, **43**, 668–698.
2 S. Burge, G. N. Parkinson, P. Hazel, A. K. Todd and S. Neidle, *Nucleic Acids Res.*, 2006, **34**, 5402–5415.
3 J. Dai, M. Carver and D. Yang, *Biochimie*, 2008, **90**, 1172–1183.
4 P. L. Tran, J. L. Mergny and P. Alberti, *Nucleic Acids Res.*, 2010.
5 D. Gomez, A. Guedin, J. L. Mergny, B. Salles, J. F. Riou, M. P. Teulade-Fichou and P. Calsou, *Nucleic Acids Res.*, 2010, **38**, 7187–7198.
6 D. Sun, K. Guo and Y. J. Shin, *Nucleic Acids Res.*, 2010, **39**, 1256–1265.
7 S. Lattmann, B. Giri, J. P. Vaughn, S. A. Akman and Y. Nagamine, *Nucleic Acids Res.*, 2010, **38**, 6219–6233.
8 S. Rankin, A. P. Reszka, J. Huppert, M. Zloh, G. N. Parkinson, A. K. Todd, S. Ladame, S. Balasubramanian and S. Neidle, *J. Am. Chem. Soc.*, 2005, **127**, 10584–10589.
9 T. S. Dexheimer, D. Sun and L. H. Hurley, *J. Am. Chem. Soc.*, 2006, **128**, 5404–5415.
10 R. J. Harrison, J. Cuesta, G. Chessari, M. A. Read, S. K. Basra, A. P. Reszka, J. Morrell, S. M. Gowan, C. M. Incles, F. A. Tanious, W. D. Wilson, L. R. Kelland and S. Neidle, *J. Med. Chem.*, 2003, **46**, 4463–4476.
11 J. H. Tan, T. M. Ou, J. Q. Hou, Y. J. Lu, S. L. Huang, H. B. Luo, J. Y. Wu, Z. S. Huang, K. Y. Wong and L. Q. Gu, *J. Med. Chem.*, 2009, **52**, 2825–2835.
12 A. Siddiqui-Jain, C. L. Grand, D. J. Bearss and L. H. Hurley, *Proc. Natl. Acad. Sci. U. S. A.*, 2002, **99**, 11593–11598.
13 T.-M. Ou, Y.-J. Lu, C. Zhang, Z.-S. Huang, X.-D. Wang, J.-H. Tan, Y. Chen, D.-L. Ma, K.-Y. Wong, J. C.-O. Tang, A. S.-C. Chan and L.-Q. Gu, *J. Med. Chem.*, 2007, **50**, 1465–1474.
14 T. Agarwal, S. Roy, T. K. Chakraborty and S. Maiti, *Biochemistry*, 2010, **49**, 8388–8397.
15 M. Bejugam, S. Sewitz, P. S. Shirude, R. Rodriguez, R. Shahid and S. Balasubramanian, *J. Am. Chem. Soc.*, 2007, **129**, 12926–12927.
16 M. Gunaratnam, S. Swank, S. M. Haider, K. Galesa, A. P. Reszka, M. Beltran, F. Cuenca, J. A. Fletcher and S. Neidle, *J. Med. Chem.*, 2009, **52**, 3774–3783.
17 X. D. Wang, T. M. Ou, Y. J. Lu, Z. Li, Z. Xu, C. Xi, J. H. Tan, S. L. Huang, L. K. An, D. Li, L. Q. Gu and Z. S. Huang, *J. Med. Chem.*, 2010, **53**, 4390–4398.
18 N. H. Campbell, G. N. Parkinson, A. P. Reszka and S. Neidle, *J. Am. Chem. Soc.*, 2008, **130**, 6722–6724.
19 S. M. Gowan, R. Heald, M. F. G. Stevens and L. R. Kelland, *Mol. Pharmacol.*, 2001, **60**, 981–988.
20 E. Gavathiotis, R. A. Heald, M. F. G. Stevens and M. S. Searle, *J. Mol. Biol.*, 2003, **334**, 25–36.
21 C. Hounsou, L. Guittat, D. Monchaud, M. Jourdan, N. Saettel, J. L. Mergny and M. P. Teulade-Fichou, *ChemMedChem*, 2007, **2**, 655–666.
22 A. D. Moorhouse, A. M. Santos, M. Gunaratnam, M. Moore, S. Neidle and J. E. Moses, *J. Am. Chem. Soc.*, 2006, **128**, 15972–15973.
23 R. T. Wheelhouse, S. A. Jennings, V. A. Phillips, D. Pletsas, P. M. Murphy, N. C. Garbett, J. B. Chaires and T. C. Jenkins, *J. Med. Chem.*, 2006, **49**, 5187–5198.

24 Z. A. Waller, P. S. Shirude, R. Rodriguez and S. Balasubramanian, *Chem. Commun.*, 2008, 1467–1469.
25 S. Neidle and G. N. Parkinson, *Biochimie*, 2008, **90**, 1184–1196.
26 S. Neidle, *Curr. Opin. Struct. Biol.*, 2009, **19**, 239–250.
27 J. Q. Hou, S. B. Chen, J. H. Tan, T. M. Ou, H. B. Luo, D. Li, J. Xu, L. Q. Gu and Z. S. Huang, *J. Phys. Chem. B*, 2010, **114**, 15301–15310.
28 G. N. Parkinson, M. P. H. Lee and S. Neidle, *Nature*, 2002, **417**, 876–880.
29 K. N. Luu, A. T. Phan, V. Kuryavyi, L. Lacroix and D. J. Patel, *J. Am. Chem. Soc.*, 2006, **128**, 9963–9970.
30 N. Zhang, A. T. Phan and D. J. Patel, *J. Am. Chem. Soc.*, 2005, **127**, 17277–17285.
31 A. Matsugami, Y. Xu, Y. Noguchi, H. Sugiyama and M. Katahira, *FEBS J.*, 2007, **274**, 3545–3556.
32 S. Chowdhury and M. Bansal, *J. Phys. Chem. B*, 2001, **105**, 7572–7578.
33 J. Sponer and N. Spackova, *Methods*, 2007, **43**, 278–290.
34 J.-L. Mergny, L. Lacroix, M.-P. Teulade-Fichou, C. Hounsou, L. Guittat, M. Hoarau, P. B. Arimondo, J.-P. Vigneron, J.-M. Lehn, J.-F. Riou, T. Garestier and C. Helene, *Proc. Natl. Acad. Sci. U. S. A.*, 2001, **98**, 3062–3067.
35 A. De Cian, L. Guittat, M. Kaiser, B. Sacca, S. Amrane, A. Bourdoncle, P. Alberti, M. P. Teulade-Fichou, L. Lacroix and J. L. Mergny, *Methods*, 2007, **42**, 183–195.
36 P. A. Rachwal and K. R. Fox, *Methods*, 2007, **43**, 291–301.
37 J.-L. Zhou, Y.-J. Lu, T.-M. Ou, J.-M. Zhou, Z.-S. Huang, X.-F. Zhu, C.-J. Du, X.-Z. Bu, L. Ma, L.-Q. Gu, Y.-M. Li and A. S.-C. Chan, *J. Med. Chem.*, 2005, **48**, 7315–7321.
38 J. Dash, P. S. Shirude, S. T. Hsu and S. Balasubramanian, *J. Am. Chem. Soc.*, 2008, **130**, 15950–15956.
39 S. Paramasivan, I. Rujan and P. H. Bolton, *Methods*, 2007, **43**, 324–331.
40 E. M. Rezler, J. Seenisamy, S. Bashyam, M.-Y. Kim, E. White, W. D. Wilson and L. H. Hurley, *J. Am. Chem. Soc.*, 2005, **127**, 9439–9447.
41 E. W. White, F. Tanious, M. A. Ismail, A. P. Reszka, S. Neidle, D. W. Boykin and W. D. Wilson, *Biophys. Chem.*, 2007, **126**, 140–153.
42 A. Ambrus, D. Chen, J. Dai, T. Bialis, R. A. Jones and D. Yang, *Nucleic Acids Res.*, 2006, **34**, 2723–2735.
43 H. Mita, T. Ohyama, Y. Tanaka and Y. Yamamoto, *Biochemistry*, 2006, **45**, 6765–6772.
44 W. C. Drewe, R. Nanjunda, M. Gunaratnam, M. Beltran, G. N. Parkinson, A. P. Reszka, W. D. Wilson and S. Neidle, *J. Med. Chem.*, 2008, **51**, 7751–7767.
45 J. Dai, C. Punchihewa, A. Ambrus, D. Chen, R. A. Jones and D. Yang, *Nucleic Acids Res.*, 2007, **35**, 2440–2450.
46 P Bates, J. L. Mergny and D. Yang, *EMBO R*, 2007, **8**, 1003–1010.
47 W. L. DeLano, *The PyMOL Molecular Graphics System (DeLano Scientific, Palo Alto, CA)*, 2002.
48 M. J. Frisch, G. W. Trucks, H. B. Schlegel, G. E. Scuseria, M. A. Robb, J. R. Cheeseman, J. A. Montgomery, Jr., T. Vreven, K. N. Kudin, J. C. Burant, J. M. Millam, S. S. Iyengar, J. Tomasi, V. Barone, B. Mennucci, M. Cossi, G. Scalmani, N. Rega, G. A. Petersson, H. Nakatsuji, M. Hada, M. Ehara, K. Toyota, R. Fukuda, J. Hasegawa, M. Ishida, T. Nakajima, Y. Honda, O. Kitao, H. Nakai, M. Klene, X. Li, J. E. Knox, H. P. Hratchian, J. B. Cross, V. Bakken, C. Adamo, J. Jaramillo, R. Gomperts, R. E. Stratmann, O. Yazyev, A. J. Austin, R. Cammi, C. Pomelli, J. Ochterski, P. Y. Ayala, K. Morokuma, G. A. Voth, P. Salvador, J. J. Dannenberg, V. G. Zakrzewski, S. Dapprich, A. D. Daniels, M. C. Strain, O. Farkas, D. K. Malick, A. D. Rabuck, K. Raghavachari, J. B. Foresman, J. V. Ortiz, Q. Cui, A. G. Baboul, S. Clifford, J. Cioslowski, B. B. Stefanov, G. Liu, A. Liashenko, P. Piskorz, I. Komaromi, R. L. Martin, D. J. Fox, T. Keith, M. A. Al-Laham, C. Y. Peng, A. Nanayakkara, M. Challacombe, P. M. W. Gill, B. G. Johnson, W. Chen, M. W. Wong, C. Gonzalez and J. A. Pople, *GAUSSIAN 03 (Revision E.01)*, Gaussian, Inc., Wallingford, CT, 2004.
49 C. M. Olsen and L. A. Marky, *Methods Mol. Biol.*, 2010, **608**, 147–158.
50 D. A. Case, T. A. Darden, T. E. C. III, C. L. Simmerling, J. W. e. al, *AMBER 10*, University of California, San Francisco, 2008.
51 I. Smirnov and R. H. Shafer, *Biochemistry*, 2000, **39**, 1462–1468.
52 J. Wang, R. M. Wolf, J. W. Caldwell, P. A. Kollman and D. A. Case, *J. Comput. Chem.*, 2004, **25**, 1157–1174.
53 Y. Duan, C. Wu, S. Chowdhury, M. C. Lee, G. Xiong, W. Zhang, R. Yang, P. Cieplak, R. Luo, T. Lee, J. Caldwell, J. Wang and P. Kollman, *J. Comput. Chem.*, 2003, **24**, 1999–2012.
54 U. Essmann, L. Perera, M. L. Berkowtz, T. Darden, H. Lee and L. G. Pedersen, *J. Chem. Phys.*, 1995, **103**, 8577–8593.
55 J. P. Ryckaert, G. Ciccotti and H. J. C. Berendsen, *J. Comput. Phys.*, 1977, **23**, 327–341.
56 P. A. Kollman, I. Massova, C. Reyes, B. Kuhn, S. Huo, L. Chong, M. Lee, T. Lee, Y. Duan, W. Wang, O. Donini, P. Cieplak, J. Srinivasan, D. A. Case and T. E. Cheatham, *Acc. Chem. Res.*, 2000, **33**, 889–897.
57 P. Hazel, G. N. Parkinson and S. Neidle, *Nucleic Acids Res.*, 2006, **34**, 2117–2127.

 This journal is © The Royal Society of Chemistry 2011